



**International
Collaboration
Center**

Institute for Materials Research
Tohoku University

ICC-IMR FY2018 Activity Report

<http://www.icc-imr.imr.tohoku.ac.jp/>

ICC-IMR FY2018

Activity Report

International Collaboration Center

Institute for Materials Research
Tohoku University

CONTENTS



Mission	02
Committee Members	03
Visiting Scholars	05
Workshops	17
Short-term Visiting Researchers	45
Young Researcher Fellowships	62



Mission

The ICC-IMR was founded in April 2008 as the center for international collaboration of the Institute for Materials Research (IMR) a center of excellence in material science, consisting of 27 research groups and five research centers. The ICC-IMR works as a gateway of diverse collaborations between overseas and IMR researchers. The ICC-IMR has invited 57 visiting professors and conducted 21 international research projects since its start-up (please inspect the graph below for more details,). The applications are open to foreign researchers and the projects are evaluated by a peer-review process involving international reviewers.

ICC-IMR coordinates five different programs:

- 1) International Integrated Project Research
- 2) Visiting Professorships
- 3) International Workshops
- 4) Fellowship for Young Researcher and PhD Student
- 5) Material Transfer Program

We welcome applicants from around the globe to submit proposals!

Visitors supported by ICC-Programs.



ICC-IMR COMMITTEE MEMBERS

Director

Prof. Gerrit E. W. BAUER

Steering Committee

Prof. Hidemi KATO

Prof. Hiroyuki NOJIRI

Prof. Hitoshi MIYASAKA

Prof. Shin-ichi ORIMO

Prof. Akira YOSHIKAWA

Prof. Masaki FUJITA

Prof. Yoshifumi ONOSE

Prof. Dai AOKI

Prof. Kozo FUJIWARA

Activity Report

Visiting Scholars



【1】Visiting Researchers

Application No.	Name	Host Professor	Proposed Research	Title	Affiliation	Term
18G01	Zhiyong Qiu	Prof. Bauer	Spin Injection and Transport of Cr ₂ O ₃ Films	Professor	Dalian University of Technology	2018.12.25-2019.3.15
18G02	Mukannan Arivanandhan	Prof. Fujiwara	Defect Engineering in SiGe Alloy Semiconductor for Thermoelectric Applications	Associate Professor	Centre for Nanoscience and Technology, Anna University, Chennai, India	2018.11.12-2019.1.30
18G03	Choi Kwang Yong	Prof. Nojiri	Searching for a Kitaev Spin Liquid in α -Ru _{1-x} Ir _x Cl ₃	Professor	Chung-Ang University, Korea	2019.1.4-2019.2.27
18G04	Mohamed Abdel-Hady Gepreel	Prof. Chiba	Advanced Characterization of New High Entropy Alloys That Show Stress-Induced Martensitic Transformation	Associate Professor	Egypt-Japan University of Science and Technology (E-JUST), Egypt	2019.2.1-2019.3.8

Electrical field controlled spin transport in antiferromagnetic Cr₂O₃

Zhiyong Qiu

Electrical spin - the key element of spintronics - has been regarded as a powerful substitute for the electrical charge in the next generation of information technology, in which spin plays the role of the carrier of information and/or energy similar to the electrical charge in electronics. Controlling of spin transport in a solid is one of the most important issues. Here, we demonstrated that spin transport can be modulated by an electrical field in an antiferromagnetic insulator Cr₂O₃.

Introduction

From the discovery of giant magneto-resistance (GMR) [1, 2], spintronics, a new branch which studies at the cross of magnetism, electronics, and informatics, has become the hotspot of the science community [3, 4]. GMR is, therefore, considered as the start point of the modern spintronics. Since the beginning of the 21st century, spintronics has grown up to be a separate research field revolving around a more fundamental keyword 'spin current', which is respected to instead the 'charge current' as the carrier of information and/or energy in the next generation spin-based information process device [5]. Here, generation, modulation, and detection of a spin current are no doubt the three central issues [6]. However, it is still far from the achievement of a real applicable spin-device, in which efficient modulation of spin current is the urgent issue.

In our previous work, it is found that the magnetic-ordering parameters are strongly coupled with the transport spin in antiferromagnetic (AFM) systems [7, 8]. Spin susceptibility and Neel vector are identified to be the most important factors for spin transport in an

AFM system. These results opened a new possibility to achieve modulate high efficient modulation of spin current in an AFM system.

In this work, we show that the transport of a spin current can be controlled by an applied bias electrical field in an antiferromagnetic insulator Cr₂O₃. This is attributed to the magnetoelectric effect of Cr₂O₃, which relates the coupling between the magnetic and the electric properties in Cr₂O₃. Also, a spin transistor is demonstrated in this work.

Experimental and set-up

As shown in Fig. 1 a, a three-terminal trilayer device is designed to consist of a heavy metal Pt layer, an AFM insulator Cr₂O₃ layer, and a permalloy (Py) layer. There are three electrodes in this trilayer device, one is on the Py layer and the other two are on the Pt layer. As shown in Fig. 1 b, spin currents are generated from Py and injected into Cr₂O₃ layer by microwave at the ferromagnetic resonance (FMR) condition which is known as spin pumping effect. Then, spin currents, transmitted through the Cr₂O₃ layer, can be converted into an electrical signal by means of inverse spin Hall effect and detected from both electrodes on the Pt layer. An applied voltage

Keywords: spin current, spintronics, spin wave

Zhiyong Qiu (Key Laboratory of Materials Modification by Laser, Ion, and Electron Beams (Ministry of Education), School of Materials Science and Engineering, Dalian University of Technology, Dalian 116024, China)
E-mail: qiuzy@dlut.edu.cn

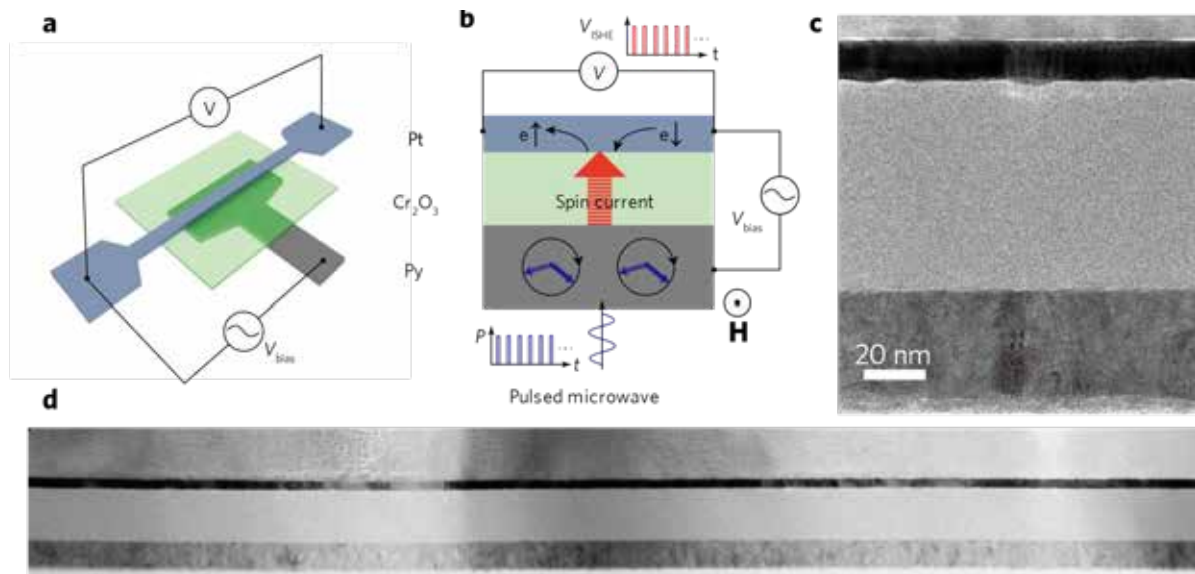


Figure 1. **a.** Set-up of spin transport experiment for the Py/Cr₂O₃/Pt trilayer device. Here, V_{bias} refer to the bias voltage between Py and Pt layers. **b.** Concept of this experiment. Spin current is generated by spin pumping effect from Py layer and injected into Cr₂O₃. Then spin current is detected by Pt layer on the other side of Cr₂O₃. The bias voltage V_{bias} is employ to control the spin transport. **c.** and **d.** show the cross section TEM image of Py/Cr₂O₃/Pt trilayer device.

between Pt and Py layers can create an out-plane electrical field in Cr₂O₃ layer, which will change the magnetic structure of Cr₂O₃ by means of magnetoelectric effect and affect the spin transport in the Cr₂O₃. Here, a pulsed microwave was used to excite the spin current in order to exclude any possible heating effects by a lock-in technique.

Both the Pt and Py layers are made from metallic targets by using an rf-sputtering system. The Cr₂O₃ layer is prepared from a sintered Cr₂O₃ target by using a pulsed laser deposition system. The trilayer device in this work behaves a continuous and well-controlled interface on a large length scale (Fig. 1 **c** and **d**). The Cr₂O₃ middle layer is more like a polycrystalline structure than a high quality single crystal-like structure (Fig. 1 **c**). The x-ray diffraction results show that the Cr₂O₃ layer displays (001)-preferential orientation.

Results and discussion

Figure 2 **a** shows spin pumping signals detected from Pt/ Cr₂O₃/Py trilayer device with various bias voltage V_{bias} at temperature $T=300$

K. At all conditions, spin pumping-like signals can be observed. At the FMR field, clear voltage peaks appear. The sign of the peak voltage V_{ISHE} is reversed by reversing the polarity of the applied magnetic field, showing that the voltage peak is due to ISHE induced by spin current pumped from the Py layer.

When a bias voltage V_{bias} is applied between Pt and Py layers, spin pumping voltage signal V_{ISHE} changed significantly (Figure 2 **a**). By applying a bias voltage $V_{bias}=0.8$ mV, the voltage peaks were suppressed by a factor of over 20%. In Fig. 2 **b**, the bias voltage V_{bias} dependence of spin pumping signal V_{ISHE} is shown. V_{ISHE} are suppressed with both positive and negative V_{bias} . V_{ISHE} shows an even symmetry to the applied bias voltage.

There seems a critical voltage at around 0.16 mV in our sample. When the bias voltage is lower than this critical voltage, the spin pumping signal is stable. When the bias voltage is higher than this critical voltage, the spin pumping signal steeply decreases first and then slowly approach

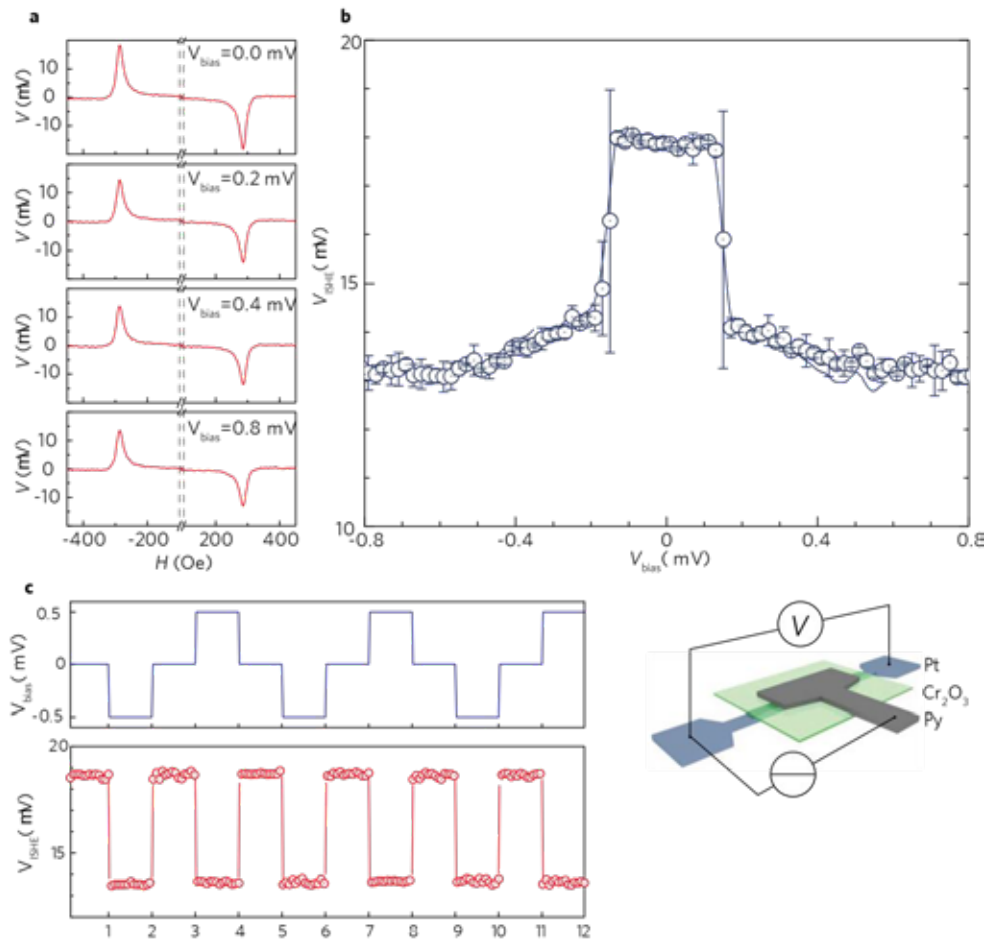


Figure 2. a. spin pumping signals in a Pt/Cr₂O₃/Py trilayer device at various bias voltages. b. The bias voltage V_{bias} dependence of inverse spin Hall voltage V_{SHE} . c. Demonstration of a spin transistor.

saturation with increasing the bias voltage.

By using the trilayer device, a spin transistor is demonstrated in Fig. 2 c. When the bias voltage is periodically switched among 0 mV and ± 0.5 mV, the spin pumping signal shows switching between high and low level, which suggest that the spin current transmission can be well controlled by an applied voltage in the Cr₂O₃.

Summary

Spin transport phenomenon in a AFM insulator Cr₂O₃ is systematically studied while an electrical field is applied. It is found that spin transmission can be well controlled by the applied bias voltage signal, and this effect can be a new approach for a spin transistor.

Reference

[1] Baibich M.N., Broto J.M., Fert Z., Van Dau F.N., Petro F., Etienne P., Creuzet G., Friederich A., and Chazelas A. Phys.

Rev. Lett. 61 2472 (1988).

[2] Binasch G., Grunberg P., Saurenbach F., and Zinn W. Phys. Rev. B 39 4828 (1989).

[3] Wolf S.A., Chtchelkanova A.Y., and Treger D.M. IBM J. Res. Dev. 50 101 (2006).

[4] Li C., Love G.D., Lyons T.W., Fike D.A., Sessions A.L., Li C., Love G.D., Lyons T.W., Fike D.A., and Sessions A.L. Science 328 80 (2016).

[5] Maekawa S., Concept in Spin Electronics (Oxford Univ. Press)

[6] Zutic I. and Das S.S. Rev. Mod. Phys. 76 323 (2004).

[7] Qiu Z., Li J., Hou D., Arenholz E., N'Diaye A.T., Tan A., Uchida K., Sato K., Okamoto S., and Tserkovnyak Y. Nat. Commun. 7 12670 (2016).

[8] Qiu Z., Hou D., Barker J., Yamamoto K., Gomonay O., and Saitoh E. Nat. Mater. 17 577 (2018).

Crystallization of $\text{Si}_{1-x}\text{Ge}_x$ alloy semiconductor during rapid cooling for thermoelectric applications

$\text{Si}_{0.7}\text{Ge}_{0.3}$ was prepared by rapid ($\sim 330^\circ\text{C}/\text{min}$) and slow cooling ($1^\circ\text{C}/\text{min}$) for thermoelectric applications. Despite of various cooling rates, the EBSD pattern revealed almost same grain structure of both samples. To understand the reason, crystal growth of $\text{Si}_{0.7}\text{Ge}_{0.3}$ sample was in-situ observed under rapid and slow cooling. The initially grown fine dendrites were re-melted and recrystallized under rapid cooling. The re-melting was not observed under slow cooling. The re-melting and recrystallization are responsible for same grain structures in the alloy.

Rapid cooling of alloys will result polycrystalline material with fine grain structures since large number of nucleation instantaneously forms under rapid cooling as observed in various alloy materials [1]. Therefore, the rapidly cooled $\text{Si}_{1-x}\text{Ge}_x$ is expected to have fine grain structures with relatively low variations of Ge composition and thereby the thermoelectric performance can be further improved. However, such kind of rapid crystallization experiments of $\text{Si}_{1-x}\text{Ge}_x$ alloy is not reported in detail except few molecular dynamics simulations of quenching of Si-Ge alloy [2]. Therefore, in the present work we have investigated the growth process of Si-rich $\text{Si}_{1-x}\text{Ge}_x$ ($x=0.1, 0.2$ and 0.3) under rapid cooling to realize the fine grain structures for high thermoelectric performance. The crystallized $\text{Si}_{0.7}\text{Ge}_{0.3}$ samples were analyzed by EDX and EBSD to study the compositional variation and grain structures.

Figure 1 shows the EBSD patterns of $\text{Si}_{0.7}\text{Ge}_{0.3}$ samples grown under rapid (a) and slow cooling (b) process. In contrast to the expectation, the grain size and structures are almost the same for both crystals even though the cooling rate in the rapid cooling experiment is more than 300 times faster than that in the slow cooling experiment.

To know the reason for the similar grain structures, crystal growth of $\text{Si}_{0.7}\text{Ge}_{0.3}$ was performed under rapid cooling and the growth process was in-situ observed using high speed microscopic camera with recorder. Further, the experiments were repeated by varying the Ge composition as 0.2, and 0.1. Moreover, the crystal growth of $\text{Si}_{1-x}\text{Ge}_x$ ($x=0.1, 0.2$ and 0.3) was performed under slow cooling with the cooling rate of $1^\circ\text{C}/\text{min}$ and the growth process was in-situ observed for comparative analysis.

Figure 2 shows the snapshots recorded during the in-situ observation of crystal growth process of $\text{Si}_{0.7}\text{Ge}_{0.3}$ and Si under rapid cooling. The first and second rows of

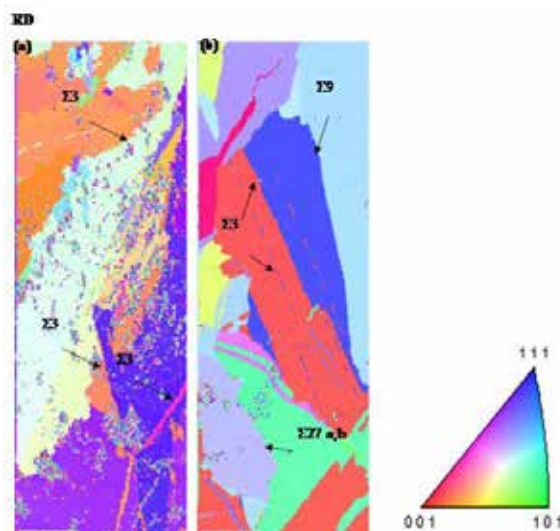


Figure 1: EBSD images of rapidly solidified (a) and slowly solidified (b) $\text{Si}_{0.7}\text{Ge}_{0.3}$ sample with colored standard triangle of orientations.

the images show the crystal growth process of $\text{Si}_{0.7}\text{Ge}_{0.3}$ at different time periods. Fine dendrites are started to grow nearly 26 seconds after shut downing the power of the heaters. The dendrites are rapidly grown for a short period of 3 seconds and started to re-melt as observed in the snapshot at 30 seconds. The re-melting is continued up to 45 seconds and completely re-melted at 50 seconds. Finally, the recrystallization is observed nearly after 70 seconds as shown in second row of Fig.2. The third row of Fig.2 show the snapshots of growth process of Si at different time periods. Two dendrites are grown under the observed area and the size of the dendrites increased with time without re-melting. From the in-situ observation experiments, it is obvious that the initially grown fine dendrites of $\text{Si}_{0.7}\text{Ge}_{0.3}$ completely re-melted under rapid cooling.

The dendrites are easily formed under rapid cooling as well as slow cooling in $\text{Si}_{1-x}\text{Ge}_x$ samples. Whereas the dendrites

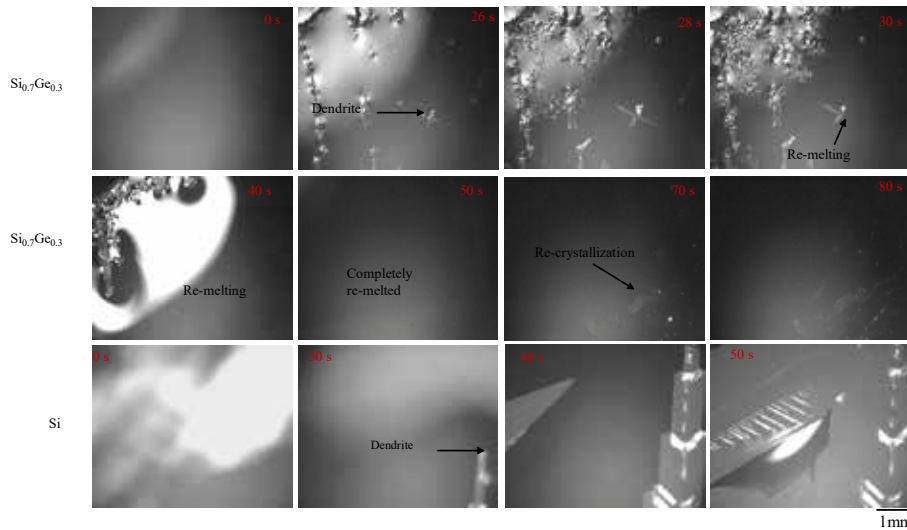


Figure 2: Snapshot images of Crystal/melt interface of $\text{Si}_{0.7}\text{Ge}_{0.3}$ and Si at different time. Re-melting is clearly indicated in the images.

are formed in Si during the rapid cooling alone and flat interface with no dendrites are observed under slow cooling. From our previous reports it is cleared that the dendrites are formed through twin boundaries [3]. The present results suggest that the formation energy of twin boundaries may be relatively low in $\text{Si}_{1-x}\text{Ge}_x$ compared to Si and thereby the dendrites are easily formed in $\text{Si}_{1-x}\text{Ge}_x$ even under slow cooling process. However, further experimental results are needed to confirm the same. Moreover, the similar grain structures of $\text{Si}_{1-x}\text{Ge}_x$ under rapid cooling as well as slow cooling is mainly attributed due to re-melting of initially grown fine dendrites and recrystallization at relatively low temperature.

References

- [1] Dollar, M.; Thompson, A.W., Acta Metall., 35 (1987) 227-235.
- [2] Treacy, M. M.; Borisenko, K. B. Science, 335 (2012) 950-953.
- [3] Fujiwara, K.; Maeda, K.; Usami, N.; Nakajima, K., Phys. Rev. Lett. 101 (2008) 055503.

List of Publications:

1. M.Arivanandhan, G. Takakura, D.Sidharth, K. Maeda, K. Shiga, H. Morito, K. Fujiwara, J. Alloy and Comp., 798 (2019) 493-499.

Keywords: Crystal growth; $\text{Si}_{1-x}\text{Ge}_x$ alloy semiconductor; dendrites
 Mukannan Arivanandhan (Crystal Physics, IMR)
 E-mail: arivucz@gmail.com
<http://www.imr.ac.jp/index.html>

Searching for a Kitaev spin liquid in α -Ru_{1-x}Ir_xCl₃

The ruthenium trichloride α -RuCl₃ has recently garnered tremendous research interest as a possible realization of the celebrated $s=1/2$ Kitaev honeycomb magnet that harbors quantum and topological spin liquids. During my research stay at the IMR, we have conducted specific heat measurements of α -Ru_{1-x}Ir_xCl₃ ($x \sim 0.2$) with a view to examining the robustness of Kitaev physics under spin vacancy. Our detailed temperature- and field-dependent specific heat data unveil a quantum-critical-like behavior for $H//$ plane and a field-induced unknown phase above 5 T for $H \perp$ plane.

The search for Kitaev quantum spin liquids and concomitantly occurring Majorana fermions is one of the most intensively pursued goals in contemporary condensed matter physics. In particular, Majorana fermions have been sought after due to their applicability to fault-free quantum computation.

In the quest for quantum spin liquids, the $s=1/2$ Kitaev model on a honeycomb lattice was proposed by Alexei Kitaev in 2006 as a new platform that hosts a quantum spin-liquid ground state and two types of Majorana fermions: itinerant Majorana fermions and Z_2 static fluxes.

Since then, an enormous amount of theoretical and experimental work has been devoted to verifying these exotic quasiparticles in Kitaev candidate materials. Because the Kitaev model is analytically solvable, it has a significant advantage in identifying thermodynamic and spectroscopic features of a spin liquid over other spin-liquid systems. Nonetheless, people have soon found that real materials contain unavoidably non-Kitaev interactions that stabilize magnetic order at low temperature while preempting an expected Kitaev spin-liquid ground state.

The detrimental effects of the non-Kitaev terms can be partly nullified by the application of an external magnetic field as well as by the introduction of spin vacancies. During my research visit to the IMR, we have explored the possibility of achieving a quantum spin liquid in the diluted α -Ru_{1-x}Ir_xCl₃.

α -RuCl₃ is closest to the Kitaev candidate materials reported so far and constitutes honeycomb lattices of octahedrally coordinated Ru³⁺ ($J_{\text{eff}}=1/2$) ions as shown in Fig. 1. α -RuCl₃ shows the zigzag antiferromagnetic order $T_N \sim 7$ K, thereby obscuring the theoretically predicted Kitaev quantum spin liquid.

One route to suppress the zigzag magnetic order is by introducing nonmagnetic impurities to α -Ru_{1-x}Ir_xCl₃ [3]. Earlier studies of α -Ru_{1-x}Ir_xCl₃ have suggested the presence of

a spin-liquid-like state in the wide range of x . Especially, α -Ru_{0.8}Ir_{0.2}Cl₃ is located in the vicinity of a quantum critical point. Considering the intriguing role of nonmagnetic impurities, a careful study of the ground state is urgently requested.

Specific heat is a powerful tool for probing low-energy magnetic excitations in quantum magnets. The high-field lab, IMR provides extreme conditions for specific heat experiments.

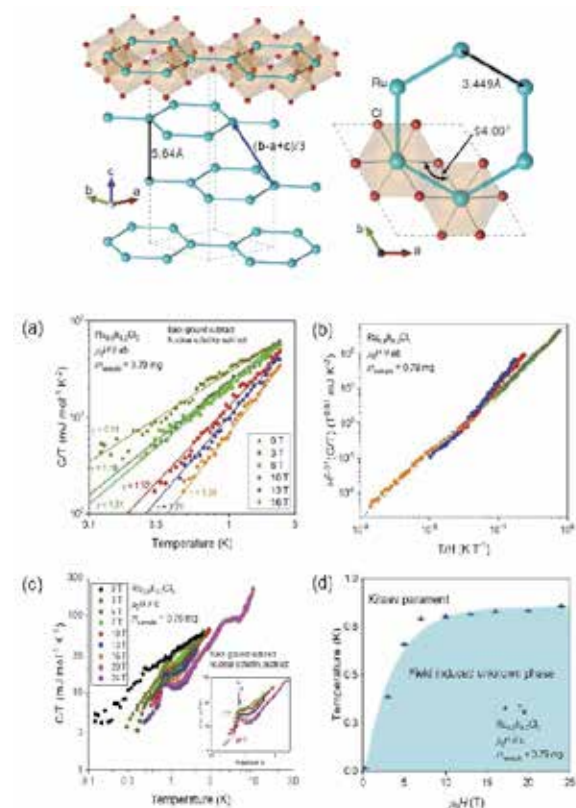


Fig. 1 (a) Specific heat plotted as C/T versus T for $H//ab$ as a function of field $\mu_0H=0-16$ T. (b) A scaling plot of $H^{0.81}(C/T)$ versus T/H . (c) C/T versus T for $H//c$ (d) T - H phase diagram of α -Ru_{0.8}Ir_{0.2}Cl₃.

We measured low-temperature specific heat using the 20 T superconducting and the 25 T Cryogen-free superconducting magnet equipped with dilution fridge and ³He cryostats. The data were taken in the

temperature range of $T=0.12-2.5$ K and the field range of $\mu_0H=0-24$ T for the external field parallel ($H//ab$) and perpendicular ($H//c$) to the honeycomb plane.

In Fig. 1(a), the low- T specific heat $C(T)$ of α - $\text{Ru}_{0.8}\text{Ir}_{0.2}\text{Cl}_3$ is plotted on the log-log scale in the in-plane fields of $\mu_0H=0-16$ T. Upon cooling in zero fields, C/T shows a power-law decrease of $C/T \propto T^{0.81}$, being close to the T dependence of what is expected for a quantum spin liquid with a Dirac node. With increasing field, the exponent gradually increases towards $C/T \propto T^{1.84}$. This suggests the presence of highly degenerate low-lying excitations around energy $E=0$. The low-energy density of states is gradually depleted with increasing field.

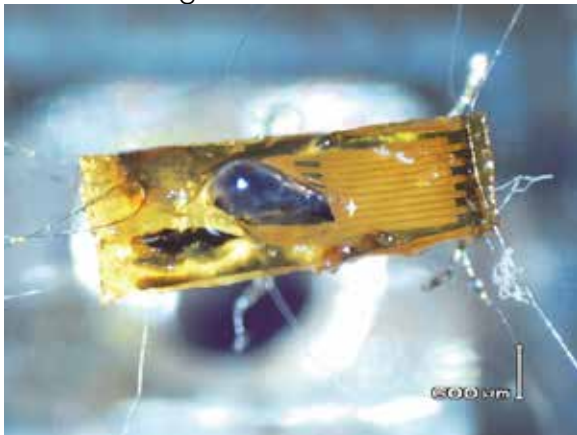


Fig. 2 An example of the sample stage for heat capacity measurement in very low temperature.

In the examination of the scaling relation, we plot $H^\alpha C/T$ vs T/H in Fig. 1(b). We find the data collapse of C/T onto a single curve over three orders of magnitude with the scaling exponent $\alpha=0.81$. The power-law scaling is

consistent with quantum-critical-like behavior. Indeed, it has been observed in a class of quantum spin liquids with bond randomness [4, 5]. At the moment, dc magnetic susceptibility and magnetization measurements are underway to crosscheck the universal quantum scaling behavior in thermodynamic quantities.

Fig. 1(c) shows the out-of-field dependence of the low- T specific heat plotted on a log-log scale of C/T vs T . With the application of the magnetic field above 5 T, the weak magnetic anomaly starts to appear at 0.7 K and slightly increases with increasing field up to 24 T. For $H//c$ the T - H phase diagram of α - $\text{Ru}_{0.8}\text{Ir}_{0.2}\text{Cl}_3$ is summarized in Fig. 1(d).

It is quite striking that the magnetic behavior relies strongly on the field-orientation direction. Possibly, this is linked to a large anisotropy of the pristine α - RuCl_3 . We have a plan for torque magnetometer experiments to draw a complete phase diagram.

In summary, our temperature- and field-dependence of the specific heat unravels a highly anisotropic magnetism of the diluted α - $\text{Ru}_{0.8}\text{Ir}_{0.2}\text{Cl}_3$. Our results suggest that α - $\text{Ru}_{0.8}\text{Ir}_{0.2}\text{Cl}_3$ is proximate to a quantum critical point. In future work, we will elucidate whether the spin-liquid-like state in α - $\text{Ru}_{0.8}\text{Ir}_{0.2}\text{Cl}_3$ has a Kitaev spin-liquid flavor.

I am grateful to Prof. Hiroyuki Nojiri and Nojiri group members for the generous support of this research project and their hospitality during my stay at the IMR. This work was supported by ICC-IMR, Tohoku University.

References

- [1] A. Kitaev, *Ann. Phys. (Amsterdam)* **321**, 2 (2006).
- [2] S.-H. Do *et al.*, *Nat. Phys.* **13**, 1079 (2017).
- [3] S.-H. Do *et al.*, *Phys. Rev. B* **98**, 014407 (2018).
- [4] K. Kitagawa *et al.*, *Nature (London)* **554**, 341 (2018).
- [5] Y.-S. Choi *et al.*, *Phys. Rev. Lett.* **122**, 167202 (2019).

Keywords: Kitaev honeycomb lattice, Spin vacancy, quantum criticality
 Prof. Kwang-Yong Choi (Department of Physics, Chung-Ang University, Korea)
 E-mail: kchoi@cau.ac.kr
 http://physics.cau.ac.kr

Advanced Characterization of New High Entropy Alloys That Show Stress-Induced Martensitic Transformation

The low-cost high entropy alloys based on the Fe-Ni-Mn-Cr-Al system showed enhanced mechanical properties through controlling the phases-constitution by alloying. The alloys were characterized using TEM, EBSD, XRD, EPMA and ThermoMaster-Z techniques to understand the internal structure and strengthening mechanisms in them.

The low-cost high-entropy $\text{Al}_{(5+X)}\text{Cr}_{12}\text{Fe}_{35}\text{Mn}_{(28-X)}\text{Ni}_{20}$ alloys ($X= 5 \text{ \& } 10$) are designed based on the thermodynamic principles to be along the fcc/(fcc+bcc)/bcc phase boundary [1]. The alloy at the (fcc+bcc)/bcc phase boundary showed apparent high spring back during compression test where stress induced martensitic transformation is expected [2]. The microstructure and mechanical properties of the alloys are investigated using advanced characterization techniques available at IMR, Tohoku University. The alloys were produced using arc melting and tested in the as-cast and cold deformed condition. Elemental mapping of the as-cast and deformed structures was conducted using electron microprobe analysis (EPMA). It was confirmed that the segregation (i.e. dendritic structure) in the as-cast alloys is increasing with increasing the Al-content in the alloy. So, the alloys at the (fcc+bcc)/bcc phase boundary seems show multi-deformation mechanism.

The high magnification EMPA analysis shown

in fig. 1.a declares the formation of submicron precipitates rich with Al, Cr and Ni elements. This precipitates is confirmed to be B2 phase impeded in bcc matrix phase through TEM investigations, as show in the diffraction pattern and dark field images in fig. 1.b.

Also, it was confirmed that the alloy produced using low-C Fe-Mn as source of Mn contains C of around 0.54 mass%. Both alloys (with C and C-free) have comparable mechanical performance, as shown in figure 2.a. The microstructure of the alloys was studied using X-ray diffraction and electron backscatter diffraction. No evidence for the stress induced transformation in both alloys (with C and C-free). In situ microstructure change with deformation is needed to confirm or deny the occurrence of stress induced transformation in the alloys. In situ SEM and TEM bending test for micro-cantilever made of the alloy is planned to be done in cooperation with Prof. Takayuki Kitamura at Kyoto University.

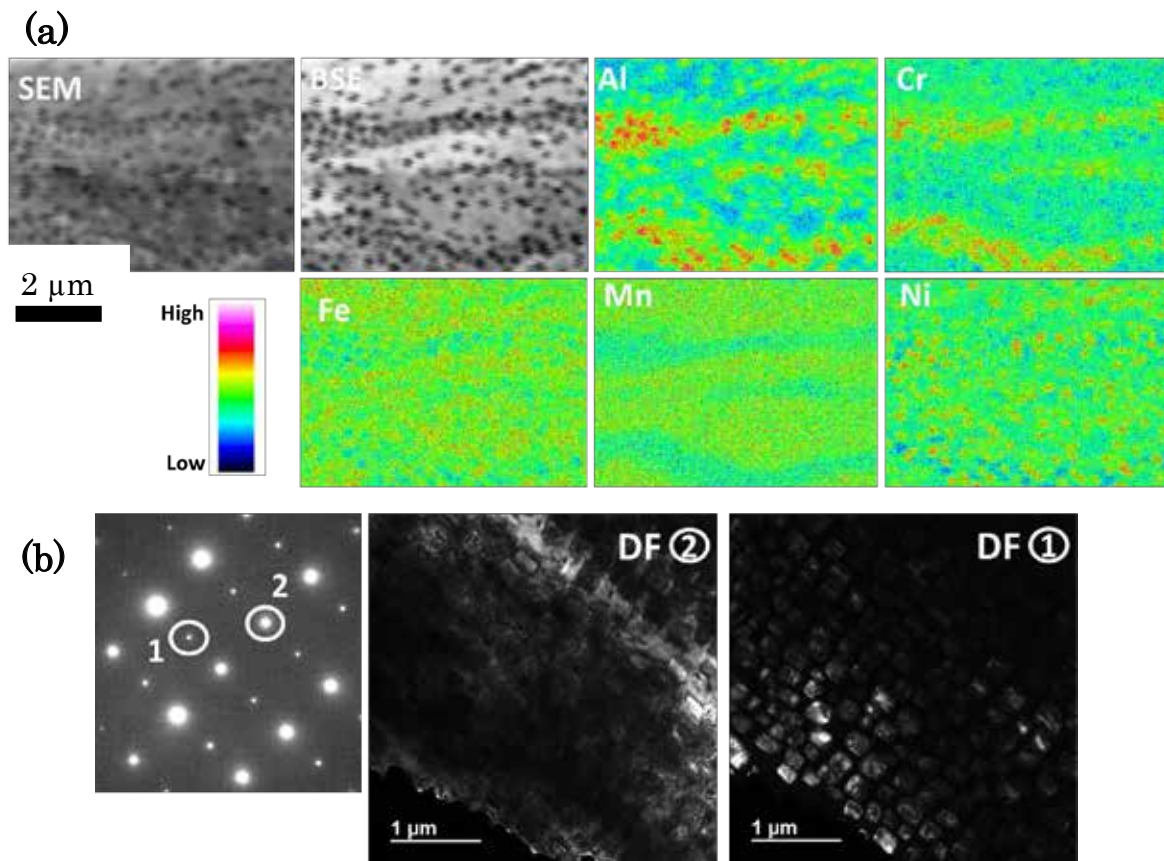


Fig.1 (a) EPMA analysis of $\text{Al}_{15}\text{Cr}_{12}\text{Fe}_{35}\text{Mn}_{18}\text{Ni}_{20}$ alloy in the as cast condition conducted at a spot size of 20 nm, and (b) TEM images (diffraction pattern, left and dark filed, DF images) of $\text{Al}_{15}\text{Cr}_{12}\text{Fe}_{35}\text{Mn}_{18}\text{Ni}_{20}$ alloy in the as-cast condition showing B2 phase (spot 1) impeded in the bcc matrix (spot 2).

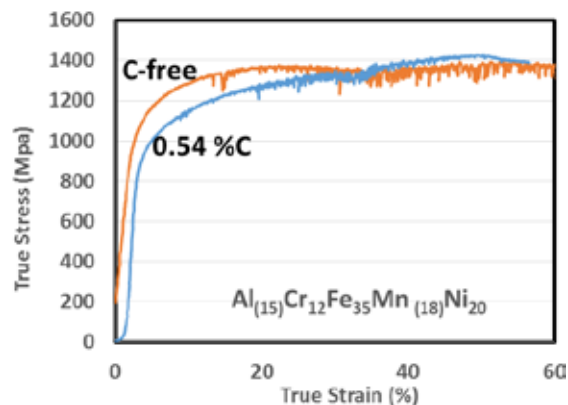


Fig.2 True stress-true strain compressive curves of the $\text{Al}_{15}\text{Cr}_{12}\text{Fe}_{35}\text{Mn}_{18}\text{Ni}_{20}$ alloys with and without 0.54 mass% C-content measured using ThermecMaster-Z technique at initial strain rate of 10^{-3} s^{-1} .

After substituting Mn with Al in $\text{Al}_5\text{Cr}_{12}\text{Fe}_{35}\text{Mn}_{28}\text{Ni}_{20}$, the yield stress of $\text{Al}_{10}\text{Cr}_{12}\text{Fe}_{35}\text{Mn}_{23}\text{Ni}_{20}$ increased by $\sim 14\%$. Moreover, the alloy maintained good cold workability and its tensile ductility exceeded

40%. Cold rolling the alloy to 90% increased its yield stress more than four times. Despite the heavy deformation caused by cold rolling (2.3 true strain), deformation twinning was induced in these alloys [3].

References

- [1] Elkhatny, S., Gepreel, M. A. H., & Hamada, A., Materials Science Forum (Vol. 917, pp. 241-245) (2018).
- [2] Han, Z. D. et.al., CHIN. PHYS. LETT. Vol. 35, No. 3, 036102 (2018).
- [3] Elkhatny, S., Gepreel, M. A., Hamada, A., Nakamura, K., Yamanaka, K., & Chiba, A., Materials Science and Engineering: A. 759. pp. 380-390 (2019).

Keywords: High entropy alloys, chemical composition, transmission electron microscopy (TEM)

Mohamed Gepreel (Department of Materials Science and Engineering, Egypt-Japan University of Science and Technology (E-JUST))

E-mail: mohamed.gepreel@ejust.edu.eg

<https://fmm.ejust.edu.eg/>

Activity Report

Workshops



【3】Workshops

Application No.	Chairpaerson	Title of Workshop	Place	Term
18WS01	Prof. Fujiwara	The 10th International Workshop on Crystalline Silicon for Solar Cells (CSSC10)	IMR Auditorium	2018.4.8-11
18WS02	Prof. Kato	13th International Workshop on Biomaterials in Interface Science	Akiu, Miyagi	2018.8.2-3
18WS03	Prof. Matsuoka	4th Intensive Discussion on Crystal Growth of Nitride Semiconductors (IDGN-4)	IMR Auditorium	2018.11.18-20
18WS04	Prof. Sasaki	Kinken-KIST Joint Symposium	IMR Auditorium	2018.7.4-5
18WS05	Prof. Fujita	HZB-IMR Workshop- Quantum Beams Researches on Materials in Extreme Conditions	HZB, Berlin	2019.3.25-26
18WS06	Prof. Kato	15th Materials Science School for Young Scientists (KINKEN-WAKATE 2018), "Dawn and Subsequent Development of the Nanomaterials": 30th Anniversary of the Nanocrystalline Soft-Magnetic Materials and Recent Progress of the Related Non-Equilibrium Nanomaterials	IMR Auditorium and Seminar Room	2018.8.29-31
18WS07	Prof. Takanashi	Summit of Materials Science 2018: SMS2018	IMR Auditorium	2018.10.29-30

The 10th International Workshop on Crystalline Silicon for Solar Cells (CSSC10)

The 10th anniversary of the international workshop on crystalline silicon for solar cells (CSSC) was celebrated in its birthplace, Institute for Materials Research, Tohoku University (Sendai, Japan), and was held from April 8th to April 11th, 2018. About 100 researchers joined to this workshop from all over the world. The participants enjoyed not only the scientific presentations including cutting edge results but also the nature and culture of Sendai and Japan during the workshop.

CSSC provides an opportunity to exchange scientific information among worldwide specialists in science and technology on crystalline Si for solar cells by especially placing emphasis on fundamental material science.

In the past, CSSC was held in Sendai (IMR), Japan (2006), Xiamen, China (2007), Trondheim, Norway (2009), Taipei, Taiwan (2010), Boston, USA (2011), Aix-les-Bains, France (2012), Fukuoka, Japan (2013), Bamberg, Germany (2015), and Tempe, USA (2016).

The 10th anniversary was celebrated in its birthplace, Sendai (IMR). Registration and reception was held at the evening on April 8. The participants enjoyed the reunion and discussion among the researchers with Miyagi's sake and light meal.



Fig. 1 Registration and reception.

Scientific lectures began on the morning of April 9 with the welcome address of Prof. Takanashi, director of IMR. In the opening session, three invited speakers gave the lectures about recent topics towards high efficiency of silicon solar cells. In the session 2, we enjoyed four lectures about the fundamentals of crystal growth for producing high-quality silicon crystals. After enjoying Japanese foods and cakes at the lunch time at SAKURA-HALL, we discussed



Fig. 2 Welcome address by Prof. Takanashi (Director of IMR).



Fig. 3 Active discussions at poster session.

the crystal growth technology of Si ingots in the session 3. After that, 36 young researchers and students gave poster presentations at the evening. We really enjoyed very active discussions in the poster session (session 4).

The third day, April 10, was a very sunny and beautiful day. In the session 5 at the morning, we learned the recent developments of recycling, sawing, and feedstock. And, the following session 6 was the special session.

Prof. Kazuo Nakajima who was the “Father” of CSSC gave a special lecture about the crystal growth of silicon. Then, the 5 researchers who are the Past Ulrich-Gösele Young Scientist Award Winners gave lectures. In the afternoon, we enjoyed Japanese and Miyagi's nature, culture, and food at the excursion and banquet. The beautiful cherry blossoms called “Hitome-Senbon-SAKURA” at Ogawara and delicious sea foods at Matsushima were the highlight other than the scientific lectures in this workshop.



Fig. 4 Beautiful SAKURA and SUNSET at excursion and banquet.

In the final day, April 11, we enjoyed scientific lectures from morning to afternoon. Novel materials for solar cells were introduced in session 7, evaluation techniques of substrates and solar cells were discussed in session 8, and advanced characterization methods were presented in the final session.

As summarized above, CSSC 10 succeeded covering a wide range of research topics from fundamental to application. 109 researchers from 15 countries participated in CSSC 10 (including 45 researchers from overseas). This indicates that CSSC born in IMR has grown to be one of the important

workshops in the field of solar cells. In the closing session, it was announced that next CSSC 11 will be held in Portugal.



Fig. 5 Participates enjoyed lectures.



Fig. 6 Meet again in Portugal!

The detail of the program of CSSC 10 is shown in the next page.

Finally, we sincerely thank ICC-IMR for their generous support.

CSSC-10 PROGRAM**April 8, Sunday**

17:00-19:00 Registration & Reception Lounge; Build#2, Institute for Materials Research, Tohoku University

April 9, Monday

8:00 Registration

Auditorium, Build#2, Institute for Materials Research, Tohoku University

Session 1: Opening Chairperson: Noritaka Usami

9:00 **Welcome address** K. Takanashi (Director, IMR, Tohoku University)

9:05 **Opening address** K. Fujiwara (Co-Chair of CSSC10, IMR, Tohoku University)

9:10 **Pushing the limits of industrial n-type wafers, solar cells and bifacial modules : efficiency and productivity** A. Jouini (CEA-INES)

9:40 **Silicon crystal growth of solar cells: Lessons learned from the pasts**
K. Kakimoto, et al. (Kyushu Univ)

10:10 **Silicon material challenges for high efficiency devices**
G. Coletti (ECN Solar Energy and UNSW)

Session 2: Crystal Growth Fundamental Chairperson: Kozo Fujiwara

11:10 **In situ X-ray based investigation of grain competition and defects during silicon crystal growth** T. Riberi-Bérédot et al. (Aix-Marseille Univ, CNRS, ESRF)

11:40 **Numerical investigations on grain evolution during direct solidification of silicon**
W. Miller et al. (IKZ, West Univ of Timisoara, Xi'an Jiaotong Univ)

12:10 **3D visualization and analysis of defects distribution in multicrystalline silicon ingot** Y. Hayama et al. (Nagoya Univ)

12:25 **In situ observation of crystal/melt interface and infrared measurement of temperature profile during solidification of silicon plate**
T. Liao, and C.W. Lan (National Taiwan Univ)

Session 3: Advanced Crystallization Chairperson: Nathan Stoddard

14:00 **Recent progress and challenges of casting technology for silicon photovoltaics**
C.W. Lan et al. (National Taiwan Univ, Solartech Energy Co.)

14:30 **Influencing the incorporation of oxygen during the directional solidification of multi-crystalline silicon by adjusting the silicon nitride coating**
S. Schwanke et al. (Fraunhofer IISB; AlzChem AG)

14:45 **Dislocation confinement by SMART approach in crystallization of G2 sized silicon ingots** P. Krenckel et al. (Fraunhofer ISE1, Nagoya Univ)

15:00 **Controlling dislocation multiplication in mono-like silicon by using <110>-oriented seeds** F. Zhang et al. (Zhejiang Univ, LDK Solar Co. Ltd)

15:15 **Development of the granulate crucible method for growth of large silicon crystals** K. Dadzis et al. (Leibniz Institute for Crystal Growth)

15:30 **An alternative Czochralski growth technique of monocrystalline silicon for high-efficiency PV cells** T. Fukuda et al. (AIST, FTB Co. LTD., Tohoku Univ)

15:45 **Reducing light induced degradation of mono silicon solar cells by using continuous Czochralski produced gallium doped silicon**
Y. Zhang et al. (Longi Green Energy Technology, GT Advanced Technologies)

Session 4: Posters 16:30-18:30

April 10, Tuesday

8:00 Registration

Session 5: Recycling, Feedstock and Sawing Chairperson: Koji Arafune

8:30 **Implementation of a circular economy based on recycled, reused and recovered indium, silicon and silver materials for photovoltaic and other applications**
N. Adamovic et al. (TU Wien, CEA)

9:00 **Thermodynamic investigations of phosphorous removal from silicon under high vacuum** G. Chichignoud et al. (Univ. Grenoble Alpes, CNRS)

9:15 **Phase diagram on carbothermic reduction of silica and alumina**
K. Itaka (Hirosaki Univ)

9:30 **Limitations to sawing of ultrathin silicon wafers by diamond multi wire saw**
B. Rynningen et al. (SINTEF Industry)

9:45 **Recovery of kerf-loss silicon from diamond wire sawing**
H.L. Yang et al. (National Taiwan Univ)

Session 6: Special Session: 10th Anniversary of CSSC

Special Commemorative Lecture by the Father of CSSC Chairperson: Chung-Wen Lan

10:20 **Growth of high quality Si ingots for solar cells using the dendritic cast method and the noncontact crucible method** K. Nakajima (Emeritus Professor, Tohoku Univ)

Lectures by the Past Ulrich-Gösele Young Scientist Award Winners

11:00 **Neogrowth silicon: a new single crystal, high purity, low oxygen bulk crystal growth method** N. Stoddard et al. (II-VI Optical Systems, Silfex, GCL, Arizona State Univ, Institute for Energy Technology, Freiburger Compound Materials)

- 11:20 **Role of crucible material and functional diffusion barrier coatings on the material quality of directionally solidified silicon ingots**
M. Trempa et al. (Fraunhofer IISB, Fraunhofer THM)
- 11:40 **Understanding the efficiency limitation of silicon material for solar cells**
M. C. Schubert et al. (Fraunhofer Institute for Solar Energy Systems, Univ of Freiburg, Univ of New South Wales, Australian National Univ)
- 12:00 **Casting industrial-scale multicrystalline silicon with ultralow carbon and ultralow dislocation density** B. Gao (The Institute of Technological Sciences, Wuhan Univ)
- 12:20 **Hydrogenated heterojunction p-type silicon solar cells with open circuit voltages > 700 mv using Czochralski and multicrystalline wafers** B. Hallam et al. (Univ of New South Wales, Arizona State Univ, Apollon Solar, FRANCE)

April 11, Tuesday

8:00 Registration

Session 7: Novel Material Chairperson: Yutaka Ohno

- 8:30 **Single crystal growth of silicon clathrate** H. Morito et al. (Tohoku Univ)
- 9:00 **Recent achievements towards high-efficiency BaSi₂ homojunction solar cells**
T. Suemasu (Univ of Tsukuba)
- 9:30 **Carrier transport in crystalline silicon heterojunction with organic thin-layer (HOT) solar cells** H. Shirai et al. (Saitama Univ)
- 9:45 **The impact of silicon contents in the aluminum paste designed for rear metallization of perc solar cells** M. Nakahara et al. (TOYO ALUMINIUM)
- 10:00 **Silicon thin foil solar cells on low cost mechanical supports**
P. Bellanger et al. (ICube, Univ of Strasbourg-CNRS, SINTEF, Department of Industrial Processes S'TILE, Faculdade de Ciências, Universidade de Lisboa/IDL)

Session 8: Fundamental Materials Science Chairperson: Wolfram Miller

- 10:45 **Superacid-derived surface passivation for measurement of ultra-long lifetimes in silicon photovoltaic materials** N. E. Grant et al. (University of Warwick, UK)
- 11:00 **Interface analysis of hydrogenated amorphous silicon passivation layer deposited by facing target sputtering** Y. Shiratori et al. (Tokyo institute of technology)
- 11:15 **Characterization of hydrogen around a-Si:H/c-Si interface by resonance nuclear reaction analysis** K. Gotoh et al. (Nagoya Univ, The Univ of Tokyo, Nagoya Institute of Technology)
- 11:30 **Insights into striations in n-type Czochralski wafers investigated via low-temperature hyperspectral and temperature-dependent spectral photoluminescence**
R. L. Chin et al. (Univ of New South Wales, Energy Research Centre of the Netherlands, Solar Energy Research Center (MIB-SOLAR), Univ of Milano-Bicocca3)
- 11:45 **Influence of dislocations in n-type CZ monocrystalline wafers on the performance of SHJ and PERT cells** M. Albaric et al. (Univ Grenoble Alpes, CEA, LITEN, DTS, LMPS, INES, Univ Grenoble Alpes, CEA, LITEN, DTS, LHET, INES, Univ Grenoble Alpes, CEA, LITEN, DTS, LHMJ, INES)
- 12:00 **Interaction of sodium atoms with stacking faults in silicon crystals with different doping levels** Y. Ohno et al. (Tohoku Univ)

Session 9: Advanced Characterization Chairperson: Martin Schubert

- 13:45 **Quantification of low-level carbon in Si by photoluminescence at liquid nitrogen temperature and higher after electron irradiation** M. Tajima et al. (Meiji Univ)
- 14:15 **Investigating defect states in monocrystalline silicon with temperature and injection dependent lifetime spectroscopy** M. S. Wiig et al. (Institute for Energy Technology, Univ of Oslo)
- 14:30 **Adaptive mapping for quick material evaluation**
K. Kutsukake et al. (Nagoya Univ, Fujitsu Laboratories, Tohoku Univ)
- 14:45 **Machine learning for recognition of etchpits on as-sliced surface of multicrystalline silicon**
T. Kojima et al. (Meiji Univ, Kyocera Corporation)
- 15:00 **Impact of the $\Sigma 9$ grain boundary structure on its electrical activity: HR-TEM and STEM investigation**
M. G. Tsoutsouva et al. (Norwegian University Science and Technology, NTNU, SINTEF Industry)

Session 10: Closing Chairperson: Kozo Fujiwara

- 15:15 **Closing remark** N. Usami, and J. M Serra

Keywords: solar cells, crystal growth, energetic material
Kozo FUJIWARA (Crystal Physics)
E-mail: kozo@imr.tohoku.ac.jp

The 13th International Workshop on Biomaterials in Interface Science

- Innovative Research for Biosis-Abiosis Intelligent Interface Summer Seminar 2018 -

The field of biosis-abiosis intelligent interface science has been developed by interdisciplinary and collaborative works, which contributes to the cognition and manipulation of phenomena arising at the interface between human constituents and biomaterials. Both researchers and students from various fields gathered at the 13th International Workshop on Biomaterials in Interface Science on Aug. 2–3rd at Sendai, Japan, where the invited lectures from 8 forefront researchers and 22 contributed oral presentations provided valuable cross-over discussions, idea communications, and new collaborations for further developing the interface science.

The development of novel biomaterials, instruments, and diagnostic techniques is crucial important for the aging society. However, phenomenon occurring in human bodies are quite complicated, because of biomaterials often require multi-functionality under various and complex circumstances. It is important to develop materials with the precise control of microstructures and interfaces in the wide scale from atomic levels to micron and larger sizes by the integration of materials and research fields. Hence, the interdisciplinary insights from a variety of scientific fields including material science, medical engineering and dentistry is required for developing novel biomaterials. Therefore interdisciplinary and international research activities are of great importance for understanding the complex phenomena and optimize the biosis-abiosis interface.

For the abovementioned purpose, three institutes in Tohoku University, including the Institute for Materials Research (IMR), Graduate School of Dentistry and Graduate School of Biomedical Engineering, have been collaborated and involved in the 5-year project related to Biomaterials, for establishing a new concept of “Biosis-Abiosis Intelligent Interface Science”. In the frame of the project, series of international forums have been held 12 times. Moreover, the 12th International Workshop on Biomaterials in Interface Science in conjunction with the Innovative Research for Biosis-Abiosis Intelligent Interface Summer Seminar 2018 was held, cooperated by a collaborative project “Creation of Life Innovation Materials for Interdisciplinary and International Researcher Development” on Aug. 2nd–3rd, 2018, at Akiu in Sendai, Japan.

This workshop had 8 invited lectures and 21 contributed oral presentations, where the invited talks were given by distinguished professors in research fields of biomedical materials from China, Korea, Indonesia, Australia, and Japan. In total, 76 participants compose of professors, researchers, and students attended. The Prof. Chuan-Bin Guo from

Peking University provided an invited talk on the development of a puncture robot for precise radioactive seed placement for treatment of tumors in the skull base. Prof. Ok-Jin Park from the Seoul National University gave an invited talk with the title of Muramyl dipeptide as a novel inducer of bone formation. Prof. Junichi Nakai from Saitama University talked about the in vivo calcium imaging with genetically encoded calcium indicators. Prof. Yin Xiao, from Queensland University of Technology gave an invited talk on the modulation of the osteoimmune environment by biomaterials for osteogenesis. Prof. Naoto Ohtake from Tokyo Institute of Technology talked “Deposition and Characterization of Diamond-like Carbon films”. Prof. Chia-Ching Wu from National Cheng Kung University gave a talk on the material and mechanical interface for peripheral nerve regeneration. Prof. Xufeng Dong from Dalian University of Technology of China talked about the mechanical properties and cytocompatibility of polymer scaffolds with anisotropic structure. Prof. Hyung-in Yoon from Seoul National University School of Dentistry gave an invited talk about the 3D-printed complete denture: in-vitro evaluation of tissue surface adaptation.

Fig.1 Shots in lectures and Group photo



Keywords: Biomedical, ceramic, metal
 Hidemi KATO (Non-Equilibrium Materials)
 E-mail: hikato@imr.tohoku.ac.jp
<http://interface2018.imr.tohoku.ac.jp/>

13th International Workshop on Biomaterials in Interface Science

Innovative Research for Biosis-Abiosis Intelligent Interface Summer Seminar 2018

Organized & Sponsored by

Creation of Life Innovation Materials for Interdisciplinary and
International Researcher Development

International Collaboration Center, Institute for Materials Research
(ICC-IMR)

<http://interface2018.imrtohoku.ac.jp/>

August 2–3, 2018

Hotel Hananoyu, Sendai, Miyagi, Japan

Workshop Agenda

2 Aug., 2018

- 13:30 Opening session
- 13:35 Session I (I-01, I-02, I-03 C-01–04) Break
- 16:20 Session II (I-04, I-05, C-05–09)
- 18:35 Group photo
- 19:30 Banquet

3 Aug., 2018

- 9:30 Session III (I-06, C-10–13)
Break
- 11:15 Session IV (I-07, C-14–17)
- 12:45 Lunch Break
- 13:45 Session V (I-08, C-18–21)

2 Aug. 2018

	Start	Time	No.		Speaker
Opening Session					
15:15	13:30	0:05		Opening address	SASAKI, Keiichi
	Closing				
Session I:					
					Chair: SASAKI, Keiichi & HANAWA, Takao
	13:35	0:30	I-01	Invited Lecture	GUO, Chuan-Bin
	14:05	0:30	I-02	Invited Lecture	HAN, Seung Hyun
	14:35	0:30	I-03	Invited Lecture	NAKAI, Junichi
	15:05	0:15	C-01	Oral talk	MATSUSHITA, Nobuhiro
	15:20	0:15	C-02	Oral talk	SATO, Emika
	15:35	0:15	C-03	Oral talk	SHIWAKU, Yukari
	15:50	0:15	C-04	Oral talk	CHIGAMA, Hiroki
	16:05	0:15		Break	
Session II:					
					Chair: SUZUKI, Osamu & KAWASHITA, Masakazu
	16:20	0:30	I-04	Invited Lecture	XIAO, Yin
	16:50	0:30	I-05	Invited Lecture	OHTAKE, Naoto
	17:20	0:15	C-05	Oral talk	TSUTSUMI, Yusuke
	17:35	0:15	C-06	Oral talk	MIYASHITA, Makiko
	17:50	0:15	C-07	Oral talk	KUROBANE, Tsuyoshi
	18:05	0:15	C-08	Oral talk	SIREGAR, Syahril
	18:20	0:15	C-09	Oral talk	YASHIRO, Wataru
	18:35			Group photo	
	19:30			Banquet	

3 Aug. 2018

Session III:					
					Chair: KATO, Hidemi
	9:30	0:30	I-06	Invited Lecture	WU, Chia-Ching
	10:00	0:15	C-10	Oral talk	TSUKAMOTO, Masahiro
	10:15	0:15	C-11	Oral talk	ABIKO, Yuki
	10:30	0:15	C-12	Oral talk	SHIBATA, Misaki
	10:45	0:15	C-13	Oral talk	SUKHBAATAR, Ariunbuyan
	11:00	0:15		break	
Session IV:					
					Chair: SAJYO, Yoshifumi
	11:15	0:30	I-07	Invited Lecture	DONG, Xufeng
	11:45	0:15	C-14	Oral talk	WU, Jun
	12:00	0:15	C-15	Oral talk	SETIANINGTYAS, Dwi
	12:15	0:15	C-16	Oral talk	QI, Jiawei
	12:30	0:15	C-17	Oral talk	KIKUCHI, Ryohei
	12:45	1:00		Lunch break	Committee Meeting
Session V:					
					Chair: TAKAHASHI, Nobuhiro
	13:45	0:30	I-08	Invited Lecture	YOON, Hyung-In
	14:15	0:15	C-18	Oral talk	WANG, Hao
	14:30	0:15	C-19	Oral talk	MIKAMI, Keita
	14:45	0:15	C-20	Oral talk	SRI, Oktamuliani
	15:00	0:15	C-21	Oral talk	KONDO, Takeru
	15:15			Closing	TAKAHASHI, Nobuhiro

4th Intensive Discussions on Growth of Nitride Semiconductors

4th Intensive Discussion on Growth of Nitride Semiconductors (IDGN-4), held on November 18-20, 2018, is aimed to analyze the status quo, and to find the direction to take in the future and the problems that need to be solved in the field of crystal growth of nitride semiconductors. To achieve these, the number of participants is limited to 50 persons including researchers from abroad, and the straightforward discussions are greatly encouraged among the selected professionals. Participants are expected to have common understandings in the current technologies and to find out the way to solve problems in the crystal growth. IDGN-4 consists of 8 technical sessions, 23 invited speakers, and 41 participants. IDGN-4 covers wide range of topics such as GaN vertical power devices, GaN-based high electron mobility transistors, device processes, defect properties, epitaxial growth technologies, bulk growth technologies, and characterization of defects.

IDGN-4 was held at Auditorium of Institute for Materials Research in Katahira campus, Tohoku University on November 18-20, 2018. About 50 specialists in the field of nitride semiconductors participated in this workshop including foreign researchers. The leading researchers in the fields of electronic devices, the crystal growth, and the characterization for devices presented each current status, and discussed on technical issues each other.

Starting from the vapor-phase growth of GaN by H. P. Marcus and J. J. Tietjen in 1969, nitride LEDs and LDs have been widely used as solid state lighting for energy saving and high-density recording such as Blu-ray, since blue LEDs became commercially available in 1996. Nitride transistors with high-frequency and high-power will come to realization in the near future. Thus, the device application has progressed in a variety of fields; however, the crystalline quality is still poor in comparison with conventional III-V semiconductors such as GaAs and InP. For the future development in high efficiency, long device-lifetime, and the expansion of application, it is indispensable to improve the crystalline quality and to control the crystal characteristics [1].

The previous workshops (IDGN-1, 2, and 3) held in 2012, 2014, and 2017 provided us the opportunity to share the most recent achievements and to discuss the technical issues on the crystal growth and device applications of nitrides. The purpose of the present workshop was to analyze the status quo, and to find the direction to take in the future and the problems that need to be solved in the field of high power and high breakdown voltage transistors, high frequency transistors [2], the epitaxial growth and the process technology for transistors [3]. Participants had common understandings in the current technologies and found out the way to solve problems in the sessions of

growth, characterization, theory, and electronic Devices. In the workshop, some selected topics were presented at the beginning of each session, for example by Prof. Srabanti Chowdhury from University of California, Dr. Leo Schowalter from Hexatech/Asahi Kasei in USA, and Dr. Malgorzata Iwinska from Institute of High Pressure Physics in Poland. The participants voluntarily presented their data, which were followed by deep and -intensive discussion. This style is not common but brought us the significant outcome.

This workshop was supported by International Collaboration Center, Institute for Materials Research (ICC-IMR), Institute for Materials Research (IMR), Institute of Multidisciplinary Research for Advanced Materials (IMRAM), Center for Collaborative Interdisciplinary Sciences, and Fukuda Crystal Laboratory Co., Ltd.

References

- [1] T. Tanikawa, K. Ohnishi, M. Kanoh, T. Mukai, and T. Matsuoka, *Appl. Phys. Express* **11**, 031004 (2018).
- [2] K. Prasertsuk, T. Tanikawa, T. Kimura, S. Kuboya, T. Suemitsu, and T. Matsuoka, *Appl. Phys. Express* **11**, 015503 (2018).
- [3] K. Ohnishi, M. Kanoh, T. Tanikawa, S. Kuboya, T. Mukai, and T. Matsuoka, *Appl. Phys. Express* **10**, 101001 (2017).



Fig. 1 Participants: selected professionals.

Keywords: nitride, crystal growth, electronic material
Takashi Matsuoka (Physics of Electronic Material, IMR)
E-mail: matsuoka@imr.tohoku.ac.jp
Workshop Website <http://www.matsuoka-lab.imr.tohoku.ac.jp/?IDGN-4>

IDGN-4 Program

November 18 (Sun)

Welcome Reception	Barbaresco, Sendai	18:00-20:00
-------------------	--------------------	-------------

November 19 (Mon)

Opening	Auditorium, Bldg. 2, IMR, Tohoku Univ.	9:00-9:15
---------	--	-----------

Electronic Devices I	Auditorium, Bldg. 2, IMR, Tohoku Univ.	9:15-10:45
----------------------	--	------------

- ED-I-1 9:15-9:45

Vertical GaN Power Devices and Automotive Application

Tetsu Kachi (Nagoya Univ., Japan)

- ED-I-2 9:45-10:15

A discussion on Vertical GaN Device Variations and their Applicability

Srabanti Chowdhury (UC Davis, USA)

- ED-I-3 10:15-10:45

Fabrication and Characterization of Vertical GaN MOSFETs

Masaaki Kuzuhara (Fukui Univ., Japan)

Break		10:45-11:15
-------	--	-------------

Electronic Devices II Auditorium, Bldg. 2, IMR, Tohoku Univ. 11:15-12:15

● ED-II-1 11:15-11:45

Mapping of Metal/Semiconductor and Semiconductor/Semiconductor Interfaces Using Scanning Internal Photoemission Microscopy

Kenji Shiojima (Fukui Univ. Japan)

● ED-II-2 11:45-12:15

Defect Electronics in SiC for High-Voltage Power Devices

Tsunenobu Kimoto (Kyoto Univ., Japan)

Lunch 12:15-13:45

Growth I Auditorium, Bldg. 2, IMR, Tohoku Univ. 13:45-14:45

● GR-I-1 13:45-14:15

Growth of GaN-Based Semiconductors on h-BN Release Layers

Yasuyuki Kobayashi (Hirosaki Univ., Japan)

● GR-I-2 14:15-14:45

Development of two-inch AlN substrates and Pseudomorphic AlGaN Technology for Optoelectronic, Power, RF, and High Temperature Applications: the Better Wide Bandgap Semiconductor Technology

Leo Schowalter (Crystal IS/Asahi Kasei, USA)

Growth II Auditorium, Bldg. 2, IMR, Tohoku Univ. 14:45-16:15

● GR-II-1 14:45-15:15

GaN Bulk Crystals by Hydride Vapor Phase Epitaxy for Power Devices

Kazuyuki Tadatomo (Yamaguchi Univ., Japan)

- GR-II-2
15:15-15:45
- Influence of different dopants on the properties of bulk GaN**

Malgorzata Iwinska (UNIPRESS, Poland)
- GR-II-3
15:45-16:15
- Recent progress of acidic ammonothermal growth of GaN**

Shigefusa F. Chichibu (Tohoku Univ., Japan)
- Break
16:15-16:45

Theory Auditorium, Bldg. 2, IMR, Tohoku Univ. 16:45-18:15

- TH-1
16:45-17:15
- Ab Initio-Based Approach to Crystal Growth of Nitride Semiconductors: Alloy Composition and Impurity Concentration**

Yoshihiro Kangawa (Kyushu Univ., Japan)
- TH-2
17:15-17:45
- Recent Progress in Computational Materials Science for Growth of Nitride Semiconductors I**

Tomonori Ito (Mie Univ., Japan)
- TH-3
17:45-18:15
- Recent Progress in Computational Materials Science for Growth of Nitride Semiconductors II: Analysis of Surfaces and Interfaces**

Toru Akiyama (Mie Univ., Japan)

Banquet The Westin Sendai 19:00-21:00

November 20 (Tue)

Electronic Devices III Auditorium, Bldg. 2, IMR, Tohoku Univ. 9:00-10:30

- ED-III-1 9:00-9:30
Prospective New Functionality of Monolithic GaN HEMT Integrated Circuits
Yasuyuki Miyamoto (Tokyo Inst. of Tech., Japan)
- ED-III-2 9:30-10:00
Low-Damage Etching for GaN-Based Electronic Devices Utilizing Photo-Electrochemical Reactions
Taketomo Sato (Hokkaido Univ., Japan)
- ED-III-3 10:00-10:30
Evaluation of Deep Levels in N-polar GaN Epitaxial Layers by Photo-Current DLTS: An Approach to Reveal the Self-Compensation Effect of Mg Doping in p-type GaN
Hiroshi Okamoto (Hirotsaki Univ., Japan)
- ED-III-4 10:30-11:00
N-polar GaN/AlGaIn Inversed High Electron Mobility Transistors
Tetsuya Suemitsu (Tohoku Univ., Japan)
- Break 11:00-11:30

Growth III Auditorium, Bldg. 2, IMR, Tohoku Univ. 11:30-12:15

- GR-III-1 11:30-12:00
AlGaIn/GaN Heterostructures Prepared by Regrowth of AlGaIn on RIE-Treated GaN and their Device Applications
Akio Yamamoto (Fukui Univ., Japan)

- GR-III-2 12:00-12:15
Effect of Polarity of GaN Substrate on AlN Formation Temperature by Substitutional Reaction between Al Layer and GaN Substrate
 Marsetio Noorprajuda (Tohoku Univ., Japan)

Lunch 12:15-13:45

Characterization Auditorium, Bldg. 2, IMR, Tohoku Univ. 13:45-15:45

- CR-1 13:45-14:15
Dislocation Properties in Bulk GaN Substrates
 Akira Sakai (Osaka Univ., Japan)
- CR-2 14:15-14:45
Revelation and Classification of Dislocations in GaN Single Crystal for Power Device Application
 Yongzhao Yao (JFCC, Japan)
- CR-3 14:45-15:15
Novel Characterization Technique of Threading Dislocations in GaN Using Multiphoton-Excitation Photoluminescence
 Tomoyuki Tanikawa (Tohoku Univ., Japan)
- CR-4 15:15-15:45
Interactions of Phonon, Electron, and Photon in Nitride Semiconductors
 Yoshihiro Ishitani (Chiba Univ., Japan)

Closing Auditorium, Bldg. 2, IMR, Tohoku Univ. 15:45-16:00

KINKEN-KIST Joint Symposium 2018

Korea Institute of Science and Technology (KIST) is a long-term partner institute of IMR. A series symposium with KIST is important for connecting researchers by exchanging the idea in the broad range of the materials science. In 2018, "KINKEN – KIST joint symposium 2018" was held in IMR.

"KINKEN - KIST Joint Symposium" was held at IMR lecture hall on 4-5 July 2018. Tohoku University has a long history of academic exchange with KIST. As a commemoration of concluding university - level academic exchange agreement between KIST and Tohoku University in 2016, Institute for Materials Research (IMR, KINKEN) and KIST jointly held a "KINKEN-KIST joint seminar" in Sendai, and that led to a series symposium in 2017 in Seoul and in 2018 in Sendai alternatively. Dr. Joonyeon Chang, director of Post-silicon Semiconductor Institute (PSI) of KIST and six young and active KIST researchers participated in this symposium by supporting from ICC-IMR.

Starting from an opening address and brief introduction of exchange history between KIST and IMR by Prof. Koki Takanashi, director of IMR, Dr. J. Chang introduced recent research activities in PSI and KIST. In the scientific sessions, wide range of research topics such as spintronics, condensed matter physics and electronic materials and device applications were presented by both KIST and IMR researches. During coffee breaks, lunch and banquet time, very vigorous discussions on each

presentation and future plan for effective exchange between KIST and IMR were conducted. In the afternoon of the second day, lab tours in IMR and group discussions were carried out.

We will deepen an academic relationship, exchange and collaboration with KIST continuously through holding this series symposium. Next symposium will be opened at KIST, Seoul in 2019.



Fig.1 Introduction talk by Dr. Joonyeon Chang, director of PSI, KIST



Fig. 2 Group photo of KINKEN - KIST symposium 2018

Keywords: spintronics, electronic materials
Takahiko Sasaki (Low Temperature condensed state physics)
E-mail: takahiko@imr.tohoku.ac.jp



Ver.180420

KINKEN-KIST joint symposium 2018

Auditorium, Institute for Materials Research, Tohoku University, Japan

July 4 (Wed) - 5 (Thu), 2018

July 3(Tue)

Hotel check-in (KIST members) Hotel Bel Air Sendai (2 min. walk from IMR) or other hotels

(Group booking by IMR office)

July 4 (Wed)

9:30-10:00 Registration

10:00-10:15 Opening remarks, Koki Takanashi (IMR)

10:15-10:30 Introduction of PSI and KIST, Joonyeon Chang (PSI, KIST)

Session 1. Spintronics I

10:30-11:00 “Current-driven creation, translation, and annihilation of ferromagnetic skyrmions observed by scanning transmission X-ray microscopy”

Jun Woo Choi (Center for Electronic Materials, PSI, KIST)

11:00-11:30 “Nonreciprocal propagation of electromagnetic waves, magnons, and acoustic waves in multiferroics”

Yoshifumi Onose (Physics of Crystal Defects Lab., IMR)

11:30-12:00 “Spintronics phenomena in topological semimetals”

Kentaro Nomura (Theory of Solid State Physics, IMR)

12:00-13:30 Lunch (Group Photo)

Session 2. Electronic materials

13:30-14:00 “Simple and scalable artificial neuron based on Ovonic Threshold Switch (OTS)”

Suyoun Lee, (Center for Electronic Materials, PSI, KIST)

14:00-14:30 “Microfabrication of functional thin films using $\text{LaAlO}_3/\text{BaO}_x$ water-soluble sacrificial templates”

Takayuki Harada (Low Temperature Physics Lab., IMR)

14:30-15:00 “Complex hydrides for all solid-state battery electrolytes”

Sangryun Kim (Hydrogen Functional Materials, IMR)

15:00-15:30 Break

Session 3. Devices and microstructure materials

- 15:30-16:00 “Three-dimensional organic field-effect transistors based on self-organization of organic semiconductor: Insulating polymer blends”
Jung Ah Lim (Center for Opto-Electronic Materials and Devices Research, PSI, KIST)
- 16:00-16:30 “Temperature effect on the microstructure of FeCo porous produced by liquid metal dealloying: its long-range ordering and transformation behavior”
Soo-Hyun, Joo (Non-Equilibrium Materials, IMR)
- 16:30-17:00 “Quantum phase transition in Electric-field-induced 2D superconductors”
Tsutomu Nojima (Laboratory of Low Temperature Materials Science, IMR)
- Reception

July 5 (Thu)

Session 4. Spintronics II

- 9:00-9:30 “Transmission line model for materials with Spin - Momentum locking”
Seokmin Hong (Center for Electronic Materials, PSI, KIST)
- 9:30-10:00 “Spin Hall effect in metallic layered structures”
Takeshi Seki (Magnetic Materials Lab., IMR)
- 10:00-10:30 “Control of spin caloritronic effects in nanostructured materials”
Masaki Mizuguchi (Collaborative Research Center on Energy Materials, IMR)
- 10:30-10:50 break

Session 5. Semiconductor Devices

- 10:50-11:20 “Low dimensional nanostructured semiconductors for electronic and optoelectronic device applications”
Do Kyung Hwang (Center for Opto-Electronic Materials and Devices Research, KIST)
- 11:20-11:50 “GaN growth and blue LED on novel oxide substrate ScAlMgO_4 ”
Shigeyuki Kuboya (Physics of Electronic Materials Lab., IMR)
- 11:50-12:00 Closing remarks, Joonyeon Chang (KIST) and Koki Takanashi (IMR)
- 12:00-13:30 Lunch
- Lab tour (High magnetic field center, other labs and research centers)

IMR-HZB workshop on material and quantum-beam sciences

IMR and HZB have agreed on a formal Memorandum of Understanding in May 2018 with the aim of promoting material science through advanced high magnetic field and quantum-beams such techniques. In the first workshop, which was held in Berlin, we exchanged information on the current status of each institute and discussed future prospects of collaboration.

The Institute for Materials Research (IMR) and the Helmholtz-Zentrum Berlin (HZB) have their long history of material science and condensed matter physics. Bearing in mind the outstanding and unique activities, especially those related to neutron scattering, high magnetic fields, and x-ray scatterings. IMR and HZB have considered the advantages that can be obtained from close cooperation in these fields of research and development and have agreed on a formal Memorandum of Understanding (MOU) in May 2018. Following subjects are listed for collaboration,

A. Materials' research using neutron scattering capabilities of IMR and HZB, including the high-field HFM-EXED facility, as well as common experiments at other neutron sources,

B. Materials research related to high magnetic field science at the high magnetic field laboratory for superconducting material at IMR,

C. High-field experiments at BESSY II synchrotron source at HZB,

D. Development of experimental capabilities for pulsed magnet experiments at the HZB synchrotron source BESSY II,

E. Sample preparation and characterization at the laboratories and facilities at IMR and at the Core-labs at HZB, and Development of sample environment for neutron and X-ray scattering experiments.

Along with this MOU, several pieces of collaborative research have been operated. For example, in September 2018, Dr. Prokhnenko visited IMR by single visit program and studies some of the magnetic oxide compounds at IMR high field laboratory. At the same time, the team has designed a compact pressure device which can be installed into 26 T high field magnet for neutron scattering at HZB. The device is under processing and will be used in experiments planned in the summer of 2019. Dr. Weschke Eugen and Prof. Nojiri, Prof. Nakamura (SPRING-8 JASRI, IMR Guest Professor in FY2018-2019) are working together to set up a compact high field



Fig. 1 The first IMR-HZB collaborative workshop was held on 25th-26th May, 2019 in Berlin. Profs. Nojiri, Fujita and Dr. Ikeda joined to the workshop from IMR.

XMCD spectrometer at BESSY II by introducing the experienced technique of high field generation of IMR group. The members of neutron group, Prof. Fujita, Dr. Nambu, and Dr. Ikeda are also collaborating with neutron scattering team of HZB for various material and are going to perform neutron spin echo measurements at HZB in 2019.

To extend existing collaborations and to launch new projects among researchers in IMR and HZB, especially relating to the science and technology at neutron instruments in the research reactor JRR-3 and at POLANO in J-PARC, Tokai, we hold the first collaborative workshop. The workshop was organized by Dr. Prokhnenko and co-workers in HZB and held on 25th and 26th March 2019 at Berlin. In the workshop, we discussed the current status of researches at each institute.

- 1) Exchange of sciences in the field of superconductivity, magnetism, and others,
- 2) Collaboration of developing high field setup in BESSY II,
- 3) Collaboration of neutron science at JRR3, transfer of techniques and

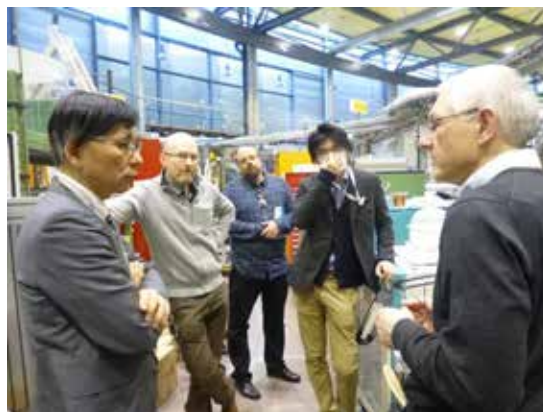


Fig. 2 View of experimental hall of BESSY II. After the workshop, we visited BESSY II. BESSY II. Is located in the Wilhelm-Conrad-Röntgen Campus of HZB, Berlin.

- knowledges of HZB, especially sample environment, to IMR spectrometers
- 4) Collaboration of development of polarized neutron devices and focusing devices and those applications to POLANO,
 - 5) Collaboration of developing multiple extreme conditions for neutron scattering,
 - 6) Science and technical cases for Soft x-ray science at synchrotron rings.

Prof. Noriji, Fujita, and Dr. Ikeda attended the workshop from IMR, and there were more than 20 participants from HZB. We confirmed the importance of collaboration between HZB and IMR. Firstly, as was announced by the Japan Atomic Energy Agency (JAEA), JRR-3 reactor will be re-operated in FY 2020 after the unexpected shut down in FY 2011 due to the Great East Japan Earthquake. IMR manages three neutron instruments (2 spectrometers and 1 diffractometer) in JRR-3. However, there is not enough resource to run all these instruments with full activity. In particular, the lack of human resources such as experienced neutron scientists is very crucial. On the other hand, Berlin reactor research reactor will be decided to close at the end of FY 2019. Therefore, if HZB members, who have excellent experiences on neutron scattering experiment, could work together with IMR members by using JRR-3 spectrometers after the shut-down of Berlin reactor, we could expect to conduct high-

level scientific researches. Such a collaborative work will be extended to future researches at POLANO in J-PARC, which is now under the commissioning phase for installing polarization devices. The second benefit of IMR-HZB collaboration is to develop x-ray scattering techniques under pulse high magnetic field at BESSY II, which is a third-generation synchrotron radiation source, and to introduce experiences of BESSY II in the planning of commitment of IMR to Tohoku synchrotron x-ray storage ring, which will be built from 2019. In IMR, there are many x-ray users who have produced various interesting results at SPring-8 and at PF of KEK. However, for the contribution of IMR to Tohoku storage ring, we need to have clear visions for constructing beam lines and spectrometers dedicated to materials sciences. In the workshop, we discuss the strategic use of synchrotron x-ray on material science. New trends of research at BESSY II were presented and several unique instruments at BESSY II were introduced in the lab. tour after the workshop. Furthermore, we met the HZB scientific director, Prof. J. Lüning to introduce IMR and discussed future prospective of IMR-HZB collaboration.

The workshop was successful as the start-up meeting of collaboration. Holding a series of meetings will contribute to extending the collaborations based on the MOU between HZB and IMR. We are going to organize the 2nd workshop in Sendai in 2020 after the shutdown of the HZB reactor.

Keywords: high magnetic field, neutron scattering, x-ray diffraction
Quantum Beam Metal Laboratory
E-mail: fujita@imr.tohoku.ac.jp
<http://qblab.imr.tohoku.ac.jp>

Workshop on

Scientific Opportunities for Materials Research using Scattering Techniques

Helmholtz-Zentrum Berlin, March 25-26, 2019

Monday, March 25, 2019 / Wannsee

Lise-Meitner-Campus (LMC), Colloquium's room, H132

Program

Time	Speaker	Title / Activity
10:00	B. Lake	Welcome
10:05	B. Lake	Experimental Investigations of Quantum Magnets at HZB
10:35	M. Fujita	Recent Activities of Neutron Research Center in IMR
11:05	K. Kiefer	Sample Environment at HZB
11:35	Y. Ikeda	Current Status of Polarized Neutron Spectrometer POLANO
12:05		<i>Lunch</i>
13:30		<i>HFM and Labs' Tour.</i> <i>Participants: H. Nojiri, M. Fujita, Y. Ikeda</i>
15:00	O. Prokhnenko	HFM/EXED Facility: Overview and Selected Scientific Examples
15:30	K. Prokes	Neutron Studies in High Magnetic Fields: Application to Uranium Systems
16:00	S. Chillal	Coupling of Charge Density Waves and Magnetism in TbTe ₃
16:30		<i>End of the first day</i>

Workshop on

Scientific Opportunities for Materials Research using Scattering Techniques

Helmholtz-Zentrum Berlin, March 25-26, 2019

Tuesday, March 26, 2019 / Adlershof

Wilhelm-Conrad-Röntgen Campus (WCRC), bldg. 13.10, room 0006 ("Kino")

Program

Time	Speaker	Title / Activity
10:00	F. Kronast	Spatially Resolved Investigation of All-optical Magnetization Switching by XPEEM
10:30	H. Nojiri	Applications of High Magnetic Fields for X-ray scattering and Spectroscopy.
11:00	E. Schierle	Resonant Soft X-Ray Scattering at UE46-PGM1: Experimental Capabilities & Selected Applications
11:30	Ch. Schüßler-Langeheine	Charge-, spin- and energy transfer on fundamental time scales: The femtoslicing laboratory at BESSY II
12:00		<i>Lunch</i>
13:30		<i>Meeting with HZB Scientific Director J. Lüning</i> <i>Participants: H. Nojiri, M. Fujita, Y. Ikeda</i>
14:00		<i>BESSY tour</i> <i>Participants: H. Nojiri, M. Fujita, Y. Ikeda</i>
15:30		<i>End of the tour; Departure to LMC</i>

KINKEN WAKATE 2018 & FINEMET 30

15th Materials Science School for Young Scientists (KINKEN WAKATE 2018) & Symposium of 30th Anniversary of Nano Crystalline Soft Magnetic Alloys (FINEMET 30) were held at IMR international center building and the auditorium on August 29-31, 2018. For providing an opportunity to learn history, fundamentals of Nano Crystalline Soft Magnetic Materials and to exchange information on own research among participants, four frontier scientists in this field were invited as lecturers.

The year 2018 was the 30th anniversary of the first paper that reported nanocrystalline soft magnetic alloys, FINEMET, by Yoshizawa et al. The importance of soft magnetic materials is still growing and further developments by young researchers are strongly expected. The aim of KINKEN WAKATE 2018 & FINEMET 30 was to learn "How did those new ideas & materials come out?" directly from the inventors or proposer of FINEMET, NANOPERM, HITPERM and Random Anisotropy Model, and to bring new idea or strategy for making something "New" to the young researcher.

KINKEN WAKATE 2018 began with an opening talk by Masato OHNUMA (Hokkaido University, Japan) and followed by four tutorial lectures.

Tutorial 1: "Fe-based nanocrystalline soft magnetic alloys and their applications" By Yoshihito YOSHIZAWA (High Energy Accelerator Research Organization (KEK), Japan)

Tutorial 2 : "Amorphous and Nanocrystalline Materials for Soft Magnetic Applications" By Giselher HERZER (Vacuumschmelze GmbH & Co. KG, Germany)



Fig. 1 Lecture by Giselher HERZER

Tutorial 3 : "Fe-M-B (M = IVa TO VIa METAL) NANOCRYSTALLINE SOFT MAGNETIC MATERIALS, A Review of Alloy Development" By Kiyonori SUZUKI (Monash University, Australia)

Tutorial 4 : "METAL AMORPHOUS NANOCOMPOSITE (MANC) MATERIALS & DEVICES FOR POWER MAGNETIC APPLICATIONS" By Michael E. MCHENRY (Carnegie Mellon University, USA)

Following to the tutorial lectures, three young researchers gave 20 minutes oral presentations on their research. Moreover, we had some students do poster presentations in the intervals.

We had 44 members of participants (9 from overseas + 35 from domestic areas), joined from 8 countries (USA, Australia, Germany, Romania, Slovakia, China, Korea and Japan). We had enthusiastic discussions and a chance to share the latest research results with the world's top scientists.



Fig. 2 Group photo

Keywords: magnetic properties, nanostructure, nucleation & growth
Hidemi KATO (Non-Equilibrium Materials division)
E-mail: hikato@imr.tohoku.ac.jp
<http://www.nem2.imr.tohoku.ac.jp/>

15th Materials Science School for Young Scientists (KINKEN WAKATE 2018) & Symposium of 30th Anniversary of Nano Crystalline Soft Magnetic Alloys (FINEMET 30)

August 29 (Wed) – 31 (Fri) 2018

Institute for Materials Research, Tohoku University, Japan

Veneu

Aug 29 – 30 : International Center of Educational Research Building, 2nd floor Seminar room 1

Aug 31 : IMR Building 2, Auditorium

Aug 29 (Wed)	KINKEN WAKATE 2018 & FINEMET 30 (International Center of Educational Research Building, 2 nd floor Seminar room 1)
16:30-17:00	Registration
17:00-17:30	(Opening talk) Masato OHNUMA, Hokkaido University, Japan "30th Anniversary of "FINEMET""

Aug 30 (Thu)	KINKEN WAKATE 2018 (International Center of Educational Research Building, 2 nd floor Seminar room 1)
9:00-10:30	(Tutorial) Yoshihito YOSHIZAWA, High Energy Accelerator Research Organization (KEK), Japan, inventor of FINEMET "Fe-based nanocrystalline soft magnetic alloys and their applications"
10:30-10:40	Break
10:40-12:10	(Tutorial) Giselher HERZER, Vacuumschmelze GmbH & Co. KG, Germany "Amorphous and Nanocrystalline Materials for Soft Magnetic Applications"
12:10-13:30	Lunch break
13:30-15:00	(Tutorial) Kiyonori SUZUKI, Monash University, Australia "Fe-M-B (M = IVa TO VIa METAL) NANOCRYSTALLINE SOFT MAGNETIC MATERIALS <i>A Review of Alloy Development</i> "
15:00-15:10	Break
15:10-16:40	(Tutorial) Michael E. MCHENRY, Carnegie Mellon University, USA "METAL AMORPHOUS NANOCOMPOSITE (MANC) MATERIALS & DEVICES FOR POWER MAGNETIC APPLICATIONS"
16:40-16:50	Break
16:50-18:05	Oral Presentation by 3 young researchers (20min+5min discussion) Markus KUHN, Technical University Darmstadt, Germany "The effect of Co addition on magnetic and structural properties of nanocrystalline (Fe,Co)-Si-B-P-Cu alloys" Sorin CORODEANU, National Institute of Research and Development for Technical Physics, Romania "Nanocrystalline glass covered microwires" Yanhui LI, Dalian University of Technology, China "Development of Fe-Si-B-Cu soft magnetic nanocrystalline alloys with high Cu concentrations"
18:30-20:30	Party : Restaurant Hagi in Tohoku Univ. Katahira campus (1,000 JPY on site)

Aug 31 (Fri)		FINEMET 30 (MR Building 2, Auditorium)
9:10-10:00	Registration	(Key note) Giselher HERZER, Vacuumschmelze GmbH & Co. KG, Germany "The Random Anisotropy Model"
10:00-10:10		Break
10:10-11:00		(Key note) Michael E. MCHENRY, Carnegie Mellon University, USA "Tunable Resistivities and Strain Induced Anisotropy in Metal Amorphous Nanocomposites with Multiple Nanocrystalline Phases"
11:00-11:10		Break
11:10-12:00		(Key note) Kiyonori SUZUKI, Monash University, Australia "Are copper and early transition metals essential for magnetically soft nanostructures?"
12:00-13:10	Lunch break	
13:10-13:40	(Invited) Shigehiro OHNUMA, Research Institute for Electromagnetic Materials, Japan "Nanogranular magnetic films for applications as high frequency soft magnets"	
13:40-14:10	(Special invited) Yoshihito YOSHIZAWA, High Energy Accelerator Research Organization (KEK), Japan, inventor of FINEMET "Development of Fe-based Nanocrystalline Soft Magnetic Alloys"	
14:10-14:45	(Invited) Ivan SKORVANEK, Slovak Academy of Sciences, Slovakia "Soft magnetic nanocrystalline bilayer ribbons for sensor applications"	
14:45-14:55	Break	
14:55-15:30	(Invited) Motoki OHTA, Hitachi Metals, Ltd., Japan "Fabrication of High B_s Fe-based nanocrystalline alloy ribbon and magnetic properties of their cores"	
15:30-16:00	(Invited) Kenji AMIYA, Tohoku University, Japan "Inverse Magnetostrictive Properties and Application of (Fe, Co)-Si-B-Nb Amorphous Alloys"	
16:00-16:35	(Invited) Nicoleta LUPU, National Institute of Research and Development for Technical Physics, Rumania "Ultrathin Nanocrystalline Magnetic Wires"	
16:35-16:45	Break	
16:45-17:10	(Oral contribution) Junji SAIDA, Tohoku University, Japan "Thermal rejuvenation in metallic glasses for improved plasticity"	
17:10-17:35	(Oral contribution) Hidemi KATO, Tohoku University, Japan "Dynamic study of primary and secondary relaxations in Pd-Ni-Cu-P glass"	
17:35-18:00	(Oral contribution) Masato OHNUMA, Hokkaido University, Japan "Role of Amorphous Phase"	

Organizing Committee:

15th Materials Science School for Young Scientists (KINKEN WAKATE 2018)

Chair: Hidemi Kato (Tohoku University)

Symposium of 30th Anniversary of Nano Crystalline Soft Magnetic Alloys (FINEMET 30)

Chair: Masato Ohnuma (Hokkaido University)

Junji Saida (Tohoku University)

Committee member

Teruo Bitoh (Akita Prefectural University)

Kiyonori Suzuki (Monash University)

Motoki Ohta (Hitachi Metals, Ltd.)

Giselher Herzer (Vacuumschmelze GmbH & Co. KG)

Kenji Amiya (Tohoku University)



Supported by

- International Collaboration Center (ICC-IMR), IMR, Tohoku University
- Creation of Life Innovation Materials for Interdisciplinary and International Research Development, Tohoku University

Summit of Materials Science 2018, October 29-30, 2018,

The Summit of Materials Science (SMS) 2018, the International general conference organized by IMR, was held on October 29th -30th. 6 Invited speakers and 14 internal speakers gave presentations on Spintronics, Magnetism, Energy-related Materials, Structural Alloys, Phase Transformation, and so on. At The end of the meetings, 72 poster presentations were given by younger researchers.



The Summit of Materials Science (SMS) is an international conference, held by the IMR and initiated after the catastrophic earthquake in 2011. It covers a broad range of topics in solid-state physics and chemistry as well as materials science. After the first conference, SMS 2016 was organized as a part of our centennial celebration. This time, IMR held the 3rd international general conference as SMS2018 on October 29th -30th.

The topics of this conference are "Spintronics and Computational Materials Science", "Materials for Energy", "Materials for Infrastructure and Analytical Science", "Materials Physics", "Chemistry and Electronics", and "Collaborating Research Facilities (Nuclear Engineering/High Magnetic field/Quantum Beam/ Industry)".

Exciting invited talks were presented by prominent speakers representative of cutting-edge researches in various fields. Moreover, professors in IMR also presented ongoing research activities in IMR. Participants were fully inspired the contents of the presentations, and many spirited discussions have been observed throughout all the sessions.



6 Invited speakers gave presentations

At the end of the conference, 72 poster presentations were given by burgeoning researchers and about 100 participants enjoyed the posters and fruitful



(Upper) Poster presentation
(Lower) Winners of Young Scientist Poster Presentation Award

Keywords: * * * * , * * * * , * * * *
Akihiko CHIBA and Masaki MIZUGUCHI (IMR Lecture committee)
E-mail: k.kouen@imr.tohoku.ac.jp
<http://www.imr.tohoku.ac.jp/kouenkai/>

Schedule of SMS2018 and IMR International Evaluation Committee

Date: Oct. 29 - 31, 2018.

Oct. 29: Day 1

International evaluation committee meeting (Venue: IMR Auditorium)

Chair: Prof. T. Kakeshita (Fukui Univ. Tech.)

10:00-11:00	Overall Performance of IMR Prof. K. Takanashi (IMR)
11:00-11:30	Discussion
11:30-13:00	Lunch & Discussion (IMR Conference Room)

SMS2018 (Venue: IMR Auditorium)

12:30-13:10 SMS 2018 Registration

13:30-15:05 Opening & Spintronics and Computational Materials Science (Chair: M. Fujita)

13:30-13:35	Prof. K. Takanashi, Welcome Address
13:35-14:05	Prof. B. Hillebrands (TU Kaiserslautern) Invited
14:05-14:25	Prof. K. Takanashi (Magnetic Materials, IMR)
14:25-14:45	Prof. G. Bauer (Theory of Solid State Physics, IMR)
14:45-15:05	Prof. M. Kubo (Materials Design by Computer Simulation, IMR)

----- Coffee Break: 15:05-15:25 -----

15:25-17:05 Materials for Energy (Chair: G. Bauer)

15:25-15:55	Prof. A. Züttel (EPFL SB ISIC LMER) Invited
15:55-16:25	Prof. T. Duffar (Grenoble INP) Invited
16:25-16:45	Prof. S. Orimo (Hydrogen Functional Materials, IMR)
16:45-17:05	Prof. A. Yoshikawa (Advanced Crystal Engineering, IMR)
17:15-18:30	Lab. Tour

----- Dinner with distinguished guests: 19:00-21:00 -----

Oct. 30: Day 2

SMS2018 (Venue: IMR Auditorium)

9:00-10:30 Materials for Infrastructure and Analytical Science (Chair: H. Kato)

09:00-09:30	Prof. N.-J. Kim (POSTECH) Invited
09:30-09:50	Prof. A. Chiba (Deformation Processing, IMR)
09:50-10:10	Prof. T. Furuhashi (Microstructure Design of Structural Metallic Materials, IMR)
10:10-10:30	Prof. T. Konno (Materials Science of Non-Stoichiometric Compounds, IMR)

----- Coffee Break: 10:30-10:50 -----

10:50-12:10 Materials Physics, Chemistry and Electronics (Chair: D. Aoki)

10:50-11:20 Prof. H. Takagi (MPI for Solid State Research) **Invited**
11:20-11:40 Prof. A. Tsukazaki (Low Temperature Physics, IMR)
11:40-12:00 Prof. T. Sasaki (Low Temperature Condensed State Physics, IMR)
12:00-12:20 Prof. H. Miyasaka (Solid-State Metal-Complex Chemistry, IMR)

----- Lunch: 12:20-13:40 -----

13:40-15:10 Collaborating Research Facilities
(Nuclear Engineering/High Magnetic field/Quantum Beam/ Industry)
(Chair: S. Awaji)

13:40-14:10 Prof. E. van Walle (SCK • CEN/KU Leuven) **Invited**
14:10-14:30 Prof. Y. Nagai (International Research Center for Nuclear Materials Science,
IMR)
14:30-14:50 Prof. H. Nojiri (High Field Laboratory for Superconducting Materials, IMR)
14:50-15:10 Prof. N. Masahashi (Cooperative Research and Development Center for
Advanced Materials, IMR)

----- Coffee Break: 15:10-15:30 -----

15:30-17:00 Poster session (Venue: IMR 2nd build. Entrance Hall)

----- SMS Exchange Party (17:30-19:30) (at IMR Lounge) -----

Oct. 31: Day 3

International evaluation committee meeting (Venue: IMR Conference Room)

9:30-11:30 Committee meeting Chair: Prof. T. Kakeshita (Fukui Inst. Tech.)

Activity Report

Short-term Visiting Researchers



【2】Short-term Visiting Researchers

Application No.	Name	Host Professor	Proposed Research	Title	Affiliation	Term
18SV01	Atsufumi Hirohata	Prof. Takanashi	Search for a Half-Metallic Antiferromagnet	Professor	University of York, UK	2018.9.16-9.27
18SV02	Valentin Taufour	Prof. Aoki	New Quantum Ferromagnets	Assistant Professor	University of California Davis, USA	2018.4.11-5.21
18SV03	Hassan Shirazi	Prof. Furuhashi	Successive Austenite Formation in Fe-18 Ni (mass%) Alloy During Intercritical Annealing	Research Associate	University of Tehran, Iran	2018.5.28-6.10
18SV04	Raza Devesh Kumar Misra	Prof. Furuhashi	Structure-Property Relationship in Advanced High Strength Steels	Professor	University of Texas at EL Paso, USA	2018.7.21-7.31
18SV05	Victor Lavin della Ventura	Prof. Yoshikawa	Study of the Pressure Effects on Emission Spectra, Band Gap Energy and Crystal Structure for Pressure Sensor Applications	Professor	University of La Laguna, Spain	2018.10.6-10.27
18SV06	Ongsa Sakthong	Prof. Yoshikawa	Growth and Characterization of (Lu, Y, Gd) ₃ (Al, Ga) ₅ O ₁₂ : Ce, Mg Crystals for Timing Application	Researcher	King Mongkut's University of Technology Thonburi (KMUTT), Thailand	2018.6.10-7.5
18SV07	Hidekazu Kurebayashi	Prof. Takanashi	Spin-Orbit Torques in Atomically-Engineered Metallic Multi-Layers	Senior Lecturer	University College London, UK	2018.10.13-10.25
18SV08	Oleksandr Prokhnenko	Prof. Nojiri	Spin Dimer Magnet SrCu ₂ (BO ₃) ₂ in High Fields	Scientist	Helmholtz-Zentrum Berlin, Germany	2018.9.15-9.27

Thermally assisted magnetisation reversal in a giant magneto-resistive junctions

In a modern computer, up to 40% of the power is wasted as heat generation, which requires cooling components. In order to utilise some of the heat generated, thermoelectric devices have been widely investigated and implemented. In this study, we have focused on the spin Seebeck effect to convert heat generated by flowing an electrical current for the operation of a magnetic tunnel junction by encapsulating with a ferromagnetic insulator, which can assist current-induced magnetisation reversal via spin wave induced by the spin Seebeck effect. This in turn reduces the critical current density for the magnetisation reversal and further reduces the total power consumption for the operation.

The spin-caloritronic effects, such as the Seebeck [1], Peltier [2] and Nernst [3] effects, are gaining significant attention due to the potential to harvest previously wasted energy in the form of heat [4]. In ferromagnetic insulators like yttrium iron garnet (YIG) or Fe_2O_3 , spin waves can be generated via the spin-Seebeck effect in the presence of a thermal gradient. For ideal efficiency this thermal gradient can be provided by the operation of the device itself via Joule heating. While the usual length scale for these gradients is micrometres, in this work a current-perpendicular-to-plane (CPP)-giant magnetoresistance (GMR) device has been insulated with Fe_2O_3 on a nanometric scale to evaluate the assistance of magnetisation reversal by a spin wave induced by the spin Seebeck effect.

A Heusler-alloy GMR multilayer, consisting of $\text{Co}_2\text{Fe}_{0.4}\text{Mn}_{0.6}\text{Si}$ (CFMS) (5)/ $\text{Ag}_{0.78}\text{Mg}_{0.22}$ (5)/CFMS (5) (thickness in nm), was grown via ultra-high-vacuum sputtering on a MgO(001) substrate with a Cr (20)/Ag (40) seed layer and was capped by Ag(2)/Au (5) layers. The seed and Heusler alloy layers were annealed at 650°C and 500°C respectively to aid crystallisation. Photo- and electron-beam lithography followed by Ar-ion milling were used to fabricate a series of elongated pillars with major axis lengths between 100 and 800 nm. As shown in Fig. 1, the milling was stopped ~1 nm into the bottom CFMS layer. For adhesion a Cr (1)/AlO (2) insulating layer was deposited underneath a 5 nm Fe_2O_3 channel around the GMR pillar.

Figure 2 shows a typical GMR behaviour for the pillars. When the field is swept from a positive to negative direction a 2.6% GMR ratio is observed, characterised by a broad rotation-controlled reversal followed by a sharper nucleation reversal. This is typical of a low-coercivity Heusler alloy such as CFMS. However, when the magnetic field is swept from negative to positive an 8% GMR signal is observed, four times greater than that in the opposite direction.

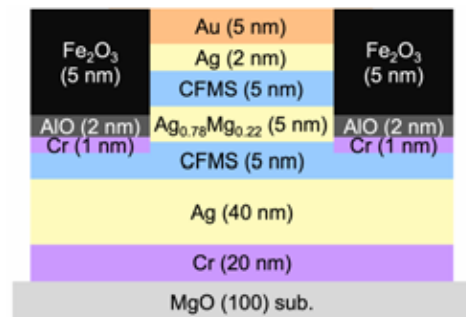


Fig. 1 Schematic of thermally assisted GMR device.

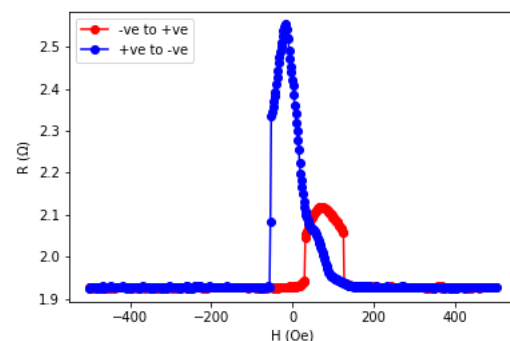


Fig. 2 Typical asymmetric GMR behaviour of spin-Seebeck enhanced GMR via Fe_2O_3 .

The current application generates a thermal gradient in the Fe_2O_3 channel via Joule heating, which in turn creates a spin-wave via the Seebeck effect. This aids the magnetisation reversal of the free layer via the stray field from the Fe_2O_3 . This thermal assistance is asymmetric due to the significant coercivity (~1 kOe) of the Fe_2O_3 layer compared to the soft Heusler alloy with coercivity <50 Oe.

The corresponding magnetisation switching induced by a current is also observed as shown in Fig. 3. We measured a clear switching along the current flowing from the bottom ferromagnet to the top ferromag-

netic layer under a small in-plane magnetic field application of 15 Oe. The current sweep starts at 0 and increases to -20 mA (red curve), indicating antiparallel to parallel magnetisation switching. The magnetisation switching is observed at 13 mA, corresponding to the switching current density of $(3\sim 10) \times 10^{-7}$ A/cm², which is almost one order of magnitude smaller than that for a similar device with the conventional AlO insulator. The current is swept to +20 (blue curve) and -20 mA (green curve) accordingly, which overlaps with each other and does not induce any magnetisation switching. This indicates that the spin wave induced by the spin Seebeck effect stabilises the magnetisation, requiring the optimisation of the pillar design for reversible operation. The critical current density for switching varies slightly, suggesting the instability of the thermally-induced spin wave in the device. This result demonstrates the magnetisation switching assisted by spin wave induced in the Fe₂O₃ insulator due to the spin Seebeck effect, which can be useful for the reduction in the power consumption of the magnetic memory operation.

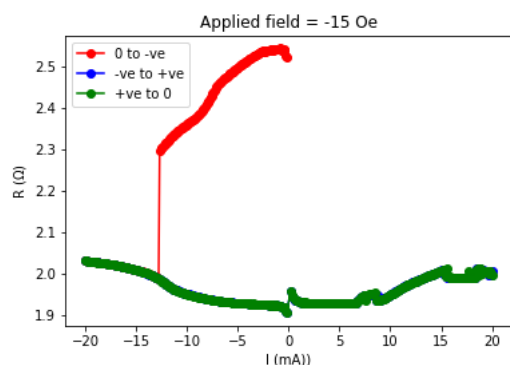


Fig. 3 Corresponding current-induced magnetisation switching behaviour of spin-Seebeck enhanced GMR via Fe₂O₃ under the in-plane magnetic field of 15 Oe.

References

- [1] K. Uchida *et al.*, *Nature* **455**, 778 (2008).
- [2] J. Flipse *et al.*, *Phys. Rev. Lett.* **113**, 027601 (2014).
- [3] S. Meyer *et al.*, *Nature Mater.* **16**, 977 (2017).
- [4] G. E. W. Bauer, E. Saitoh and B. J. van Wees, *Nature Mater.* **11**, 391 (2012).

Keywords: spin current, spin wave, oxide
Atsufumi Hirohata (University of York)
E-mail: atsufumi.hirohata@york.ac.uk
<http://www-users.york.ac.uk/~ah566/>

Ferromagnetic quantum criticality: emergence of modulated magnetic phases and spin reorientation

During this program, we successfully synthesized single crystals of two systems: CeRh_3B_2 and $\text{UFe}_{10}\text{Si}_2$. Our initial characterizations indicate that these systems are ideal candidates to study two possible outcomes of the suppression of ferromagnetism. Namely, we investigate the emergence of modulated magnetic orders in CeRh_3B_2 with Ru substitutions, and spin reorientation tri-criticality with field aligned along the hard axis in $\text{UFe}_{10}\text{Si}_2$.

When a paramagnetic-ferromagnetic phase transition is suppressed by a clean tuning parameter such as pressure, particle-hole excitations either induce the transition to become of the first order [1], or they induce the appearance of new modulated magnetic phases [2]. These phases have small magnetic wavevector q and can correspond to helical or conical orders. On the other hand, when using chemical substitutions, the introduction of disorder can reduce long wavelength correlations and the transition may remain of the second order until being suppressed at a ferromagnetic quantum critical point [3]. It is therefore difficult to identify a system which can be tuned by chemical substitutions without suppressing the effect of particle-hole excitations. Here, we introduce the system $\text{Ce}(\text{Rh}_{1-x}\text{Ru}_x)_3\text{B}_2$ which appears to be a promising system to observe the appearance of modulated magnetic phases near the suppression of ferromagnetism.

CeRh_3B_2 orders ferromagnetically below $T_C=115$ K [4] and has attracted the attention as the Ce magnet with the highest Curie temperature among Ce systems with non-magnetic elements. Studies of polycrystalline samples with Ru substitutions showed that T_C is suppressed near $x=0.08$ and a so-called “complex order” is observed in the range $0.1 < x < 0.4$ [5]. The phase diagram is shown in Fig.1a. A complex antiferromagnetic structure was proposed, but the nature of the samples (polycrystalline) did not motivate further investigations. During this program, we succeeded in synthesizing single crystals of $\text{Ce}(\text{Rh}_{0.8}\text{Ru}_{0.2})_3\text{B}_2$ using the Czochralski technique. Our magnetization measurements confirm an antiferromagnetic transition (sharp anomaly near $T_N=70$ K in Fig.1b) with the c-axis being the easy magnetization axis. However, the magnetization does not decrease significantly below T_N and increases again upon cooling below 20 K. This could be characteristic of a helical or conical type of magnetic order, as predicted to appear

near the suppression of ferromagnetism [3]. In the near future, we will perform specific heat and magnetoresistance measurements to quantify the remaining entropy at low temperature, neutron scattering experiments to clarify the magnetic order, and NMR measurements to investigate the spin fluctuations. Our work will establish that chemical substitutions in CeRh_3B_2 do not introduce much disorder, demonstrating that CeRh_3B_2 is an ideal system to study the suppression of ferromagnetism and the emergence of modulated magnetic phases.

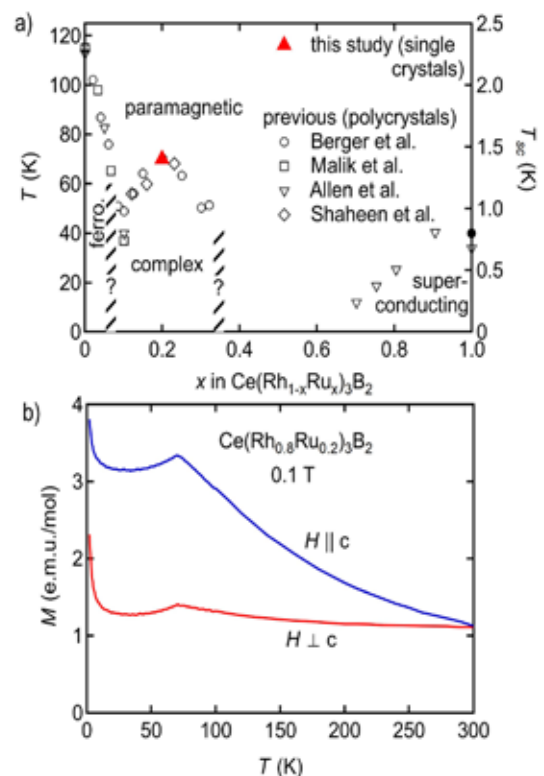


Figure 1: a) Phase diagram of $\text{Ce}(\text{Rh}_{1-x}\text{Ru}_x)_3\text{B}_2$ from polycrystalline samples b) Temperature dependence of the magnetization measured on our single crystal.

Besides pressure and chemical substitutions, another useful tuning parameter is the magnetic field. The application of a magnetic field breaks the time-reversal symmetry and smears out a

second-order paramagnetic-ferromagnetic transition. However, when the transition is of the first order, the magnetic field will induce a metamagnetic transition which eventually become a crossover at high-temperatures leading to a so-called “wing-structure” phase diagram [1,3]. Interestingly, in systems with strong magnetic anisotropy, the magnetic field can be used to suppress the paramagnetic-ferromagnetic transition even when it is of the second order, providing that the field is applied along the hard magnetization axis. As the field is increased, the transition eventually becomes of the first order before being completely suppressed at a quantum phase transition. Re-entrant superconductivity has been observed near such quantum phase transition in UCoGe and URhGe (it is possible that the metamagnetic transition in UTe₂ is of the same nature). One difficulty in studying the effect of magnetic field in these systems is that the anisotropy is very large while T_c is relatively small, which requires large magnetic fields (~11-35 T) and very low temperatures (~100 mK). In this program, we identified a system with a moderate magnetic anisotropy, but a very large Curie temperature: UFe₁₀Si₂.

UFe₁₀Si₂ has a Curie temperature of 653 K [6]. First principle calculations as well as existing data indicate a magnetic anisotropy energy between 2 and 3 MJ/m³: the moments are aligned along the c axis, and a metamagnetic jump is observed near 3-4 T when the field is applied along the a axis. In this program, we attempted to grow single crystals using the Czochralski technique. Several grains tend to nucleate during the synthesis, but we were able to isolate several samples with good crystallinity.

Our preliminary characterization measurements demonstrate that we can track the metamagnetic transition in the magnetoresistance (Fig.2): a sharp drop is observed near 3.7 T when the field is applied along the a-axis. With increasing the temperature, the transition clearly broadens, as visible by comparing measurement at 2 K

and 300 K for example. This indicates that there is a change of nature of the transition, probably from first order at low temperatures to second order at high temperatures. Indeed, when the transition is of the second order, it will be very sensitive to the alignment of magnetic field and remain sharp only if the field is precisely perpendicular to the c-axis. In the near future, we need to perform more precise measurements to identify the location of a tri-critical point where the transition changes from second to first order. Our work will establish a rare example of a spin-reorientation tri-critical point at low field and high temperature. Such system provides a key playground to investigate the physics behind the tri-critical point and enable comparison with systems with re-entrant superconductivity.

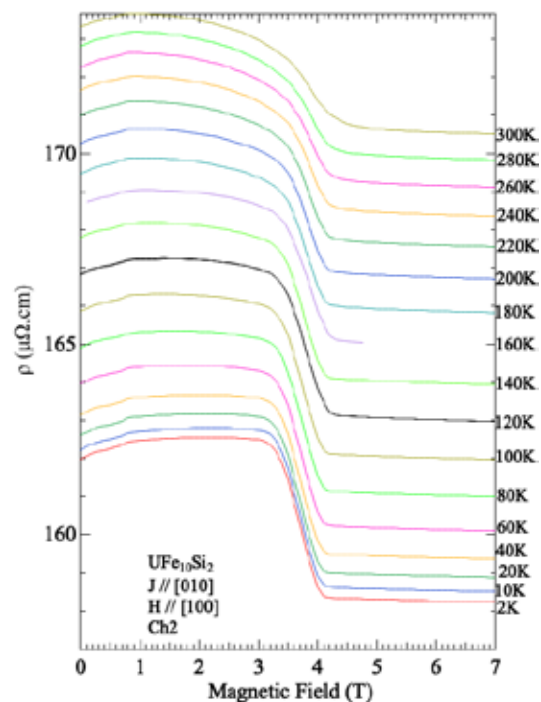


Figure 2: Magnetic field dependence of the electrical resistivity of UFe₁₀Si₂ at different temperatures with the field applied along the a-axis.

Keywords: ferromagnetic, Czochralski growth, magnetoresistance

Full Name: Dai Aoki (IMR Tohoku University) and Valentin Taufour (Department of Physics, University of California Davis)

E-mail: aoki@imr.tohoku.ac.jp and vtaufour@ucdavis.edu

References

- [1] V. Taufour, D. Aoki, G. Knebel, and J. Flouquet *Phys. Rev. Lett.*, 105, 217201, 2010.
- [2] V. Taufour, et al., *Phys. Rev. Lett.*, 117, 037207, 2016.
- [3] M. Brando, D. Belitz, F.M. Grosche, and T. R. Kirkpatrick, *Rev. Mod. Phys.*, 88, 025006, 2016.
- [4] S. K. Dhar, S. K. Malik, and R. Vijayaraghavan *Journal of Physics C: Solid State Physics*, 14, 11, L321, 1981.
- [5] S. Berger, et al., *Phys. Rev. B*, 64, 134404, 2001.
- [6] A. Andreev, S. Zadvorkin, and E. Tarasov, *J. Alloys Compd.*, 189, 2, 187, 1992.

Successive Austenite Formation in Fe-18 Ni (mass%) Alloy During Intercritical Annealing

Microstructure change at a temperature near to the upper boundary of two phase ($\alpha+\gamma$) region was studied. At the early stage, a fine lamellar structure consists of precipitated austenite and initial martensite is formed. By further holding, new austenite grains nucleated and grew at the expense of the lamellar aggregate.

Reverse transformation of the Fe-18 Ni alloy was studied during isothermal holding in upper phase boundary of the two phase region.

It was found that a lamellar aggregate consisting of precipitated austenite laths and initial martensite is formed at the early stage. By further holding new austenite grains nucleate independently and grow at the expense of lamellar aggregate. An EPMA of the specimen annealed at 863 K for 240 min is shown in Fig. 1 which demonstrates the distribution of Ni atom in the lamellar aggregate and large white area. In lamellar region, enrichment of reversely formed austenite by Ni is pointed out which clearly indicates that the austenite laths are formed by a diffusional transformation mechanism. Neighboring tempered martensite has been depleted of Ni atoms conversely. However, the large white area shows a uniform distribution of Ni concentration.

EBSD analysis of a specimen isothermally reverted at 873 K and 863 K reveal that the lamellar area shows a near KS pattern while when the large white area is incorporated to the analysis, the orientations deviate from the KS orientation relationship.

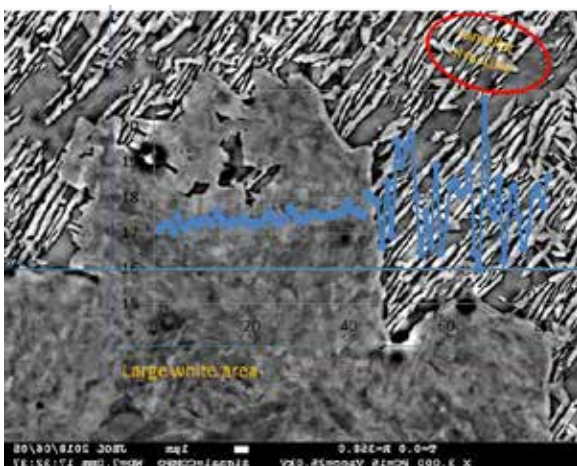


Fig. 1 EPMA analysis of Ni distribution after reverse transformation at 863 K and holding for 240 min.

Austenite in large white area has some similar characteristics of massive transformation such as partitionless without any specific orientation relationship [1, 2, and 3]. However, the transformation involves essentially a diffusion mechanism leading to the uniform distribution of Ni atoms unlike the massive transformation which is defined by interface-controlled diffusional phase transformation. Therefore, a discontinuous dissolution mechanism of transformation could be assumed for the formation of new austenite grains in which accelerated interfacial diffusion plays the main role. According to the binary Fe-Ni phase diagram, the equilibrium state of the Fe-18 Ni alloy at 873 K and 863 K consist of ferrite and austenite. The relative amount of reverted

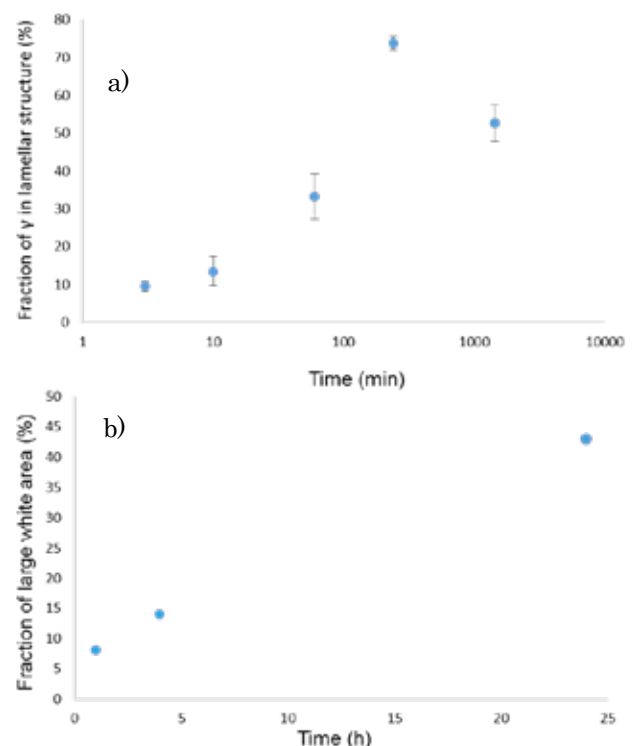


Fig. 2 Fraction of austenite during holding at 873 K for various time; a) austenite in lamellar area b) austenite in large white area

austenite at 873 K was calculated about 98 %. At the earlier stages of reversion treatment, relative amount of ferrite is higher than the equilibrium state and, therefore, the relative amount of ferrite decreases during isothermal holding which is practically accompanied by increasing of the relative amount of reversed austenite. The kinetics of this phase change should be controlled by the partitioning of Ni atoms which is expected to be rather slow due to the partial coherency of KS related martensite/austenite interfaces. Fig. 2 shows the fraction of precipitated austenite in lamellar area and new single phase as denoted by large white area in Fig. 1. Fraction of precipitated austenite increased by holding time and then decreased after 1440 min of holding. This can be related to the expense of lamellar aggregate by formation of new austenite grains at large white area.

A single phase austenite is formed in the large white region despite the fact that present treatment condition is located in the two phase region. Thermodynamics assessment is applied to interpret the peculiar features of this transformation which is demonstrated in Fig. 3, where G^{γ} and $G^{(\alpha+\gamma)}$ are the molar Gibbs free energy of large white area and the lamellar aggregate respectively. It is found out that the difference between free energy of lamellar and single phase austenite ($G^{(\alpha+\gamma)} - G^{\gamma}$) is very low for the present condition. However, remarkable interfacial energy is elaborated due to the formation of lamellar aggregate which acts as a driving force of transformation. This phenomena can be important for experimentally calculation of coherent interfacial energy as the transformation is assisted by interfacial energy.

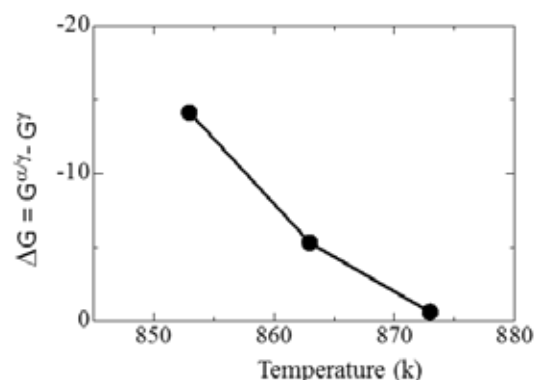


Fig. 3 Thermodynamic assessment of free energy change during reverse transformation of Fe-18Ni alloy.

References

- [1] A. Brogenstam, M. Hillert, *Acta Mater.*, 48 (2000) 2765.
- [2] H.I. Aaronson, *Metall. Mater. Trans.*, 33A (2002) 2285.
- [3] T.B. Masalski, *Metall. Mater. Trans.*, 33A (2002) 2277.

Discussion on Structure-Property Relationship in Advanced High Strength Steels

Nanograined (NG) materials exhibiting “high strength-high ductility combination” are excellent vehicles to obtain an unambiguous understanding of deformation mechanisms. Toward this end, the concept of phase reversion-induced NG structure enabled high strength-high ductility combination to be obtained. Utilizing this concept, our aim is to fundamentally understand grain size dependence on deformation mechanisms.

During the visit, a presentation was made to obtain “high strength-high ductility” combination in nanograined (NG) austenitic stainless steel. using the concept of phase reversion involving severe cold deformation of austenite at room temperature to generate strain-induced martensite, followed by annealing when martensite reverts to austenite via diffusional mechanism. The objective of the presentation was to stimulate discussion on dependence of grain size on deformation mechanisms in nanostructured steels. We also discussed the application of depth-sensing nanoindentation experiments and post-mortem analyses of the deformed region using transmission electron microscopy (TEM) in the understanding of deformation mechanisms. It was emphasized that strain rate sensitivity of the nanograined (NG) austenitic steel as obtained by nanoindentation experiments was (0.13), which is about twice the coarse-grained counterpart (0.06) and the activation volume was about one-third ($16 b^3$) of the coarse-grained structure ($48 b^3$), where b is the magnitude of the Burgers vector. In the high strength nanograined steel,

deformation twinning contributed to excellent ductility, while in the low strength coarse-grained (CG) steel, ductility was also good, but due to strain-induced martensite, implying clear distinction and fundamental transition in the deformation behavior of NG and CG Fe-17Cr-7Ni austenitic stainless steels. In the NG structure, there was marked increase in stacking faults and twin density at high strain rates, which led to decrease in the average spacing between adjacent stacking faults, converting stacking faults into twins. The plastic zone in the NG structure resembled a network knitted by the intersecting twins and stacking faults. The observed change in the deformation mechanism with change in grain size is attributed to increased stability of austenite with decrease in grain size, and is explained in terms of austenite stability-strain energy relationship [1].

The fracture surface of the CG alloy that experienced strain-induced martensitic transformation during tensile deformation was microvoid coalescence-type, which is typically observed in ductile metals and alloys. In contrast, the fracture surface of the NG alloy though

appeared relatively flat but at higher magnification it was observed that

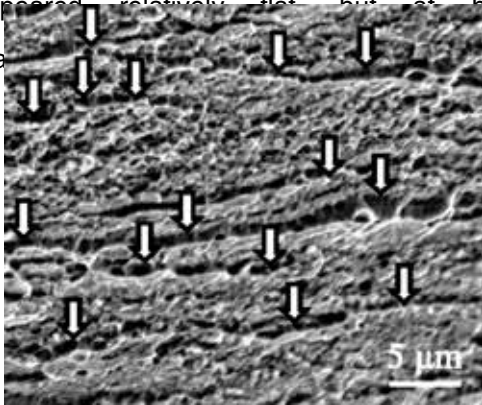


Figure 1. Striated fractured induced by twinning in nanograined austenitic stainless steel.

were nearly parallel to one another were observed with line-up of voids along the striations (Figure 1).

A strong discussion took place on the ongoing research being conducted by the members of Professor Furuwara's group.

[1] R.D.K. Misra, V.S.Y. Injeti and M.C. Somani, "The Significance of Deformation Mechanisms on the Fracture Behavior of Phase Reversion-induced Nanostructured Austenitic Stainless Steel," *Scientific Reports – Nature*, 8:7908 (2018) 1-13.

Keywords: nanostructure, electron microscopy, deformation

! Full Name: Devesh Misra
E-mail: dmisra2@utep.edu

<http://engineering.utep.edu/materials/>

Study of the Pressure Effects on Emission Spectra, Band Gap Energy and Crystal Structure of Nd³⁺-doped Garnets for Pressure Sensors

Matter under extreme pressure conditions is the subject of multidisciplinary studies that join diverse fields as physics, chemistry, geology, material science, microbiology, or food technology. The high pressure technique applied to rare earth ions in crystalline garnets provides a unique insight into the electronic structure and luminescence properties of the optically active ion. This study is focused on the possible applications of Nd³⁺ luminescence in garnets in optical pressure sensing.

Nd³⁺-doped RE₃(AlGa)₅O₁₂ (RE=Gd,Y,and Lu) crystalline garnets have been synthesized by a μ -pulling technique [1]. With the decrease of the RE atom size and the relative concentrations of Al³⁺ and Ga³⁺ ions, the chemical pressure related to the decreasing volumes of the (Al,Ga)O₄ tetrahedral, (Al,Ga)O₆ octahedral and REO₈ dodecahedral units drive the garnets toward a more compacted structure, while changing the band gap structure.

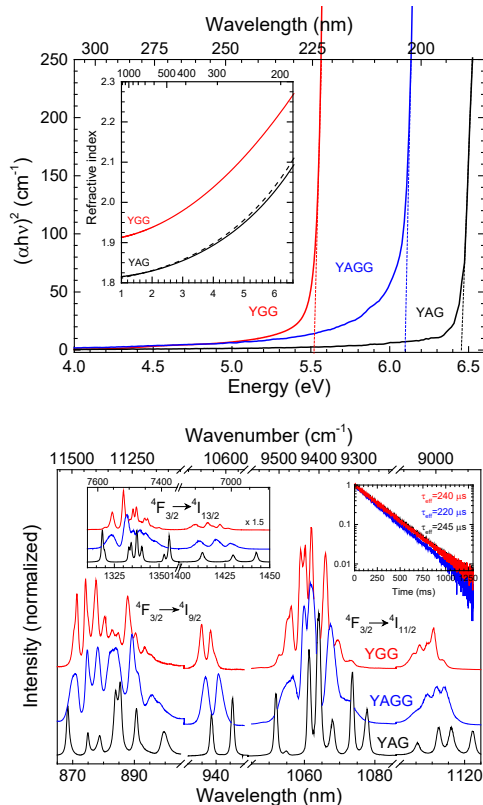


Fig. 1 (Up) Tauc-plot of the fundamental absorption edges of different garnets and (Bottom) emission spectra and lifetimes of YAG, YAGG and YGG garnets at ambient conditions.

The application of hydrostatic pressure in a diamond anvil cell (DAC) also increases the crystal-field strength felt by the RE³⁺ ions

while decreases the orthorhombic distortion of the REO₈ local environment and varies the fundamental absorption edge of the crystals. These effects alter the absorption and emission properties of the Nd³⁺ ion measured in the near-infrared associated with the $^4F_{3/2} \rightarrow ^4I_{9/2-13/2}$ transitions.

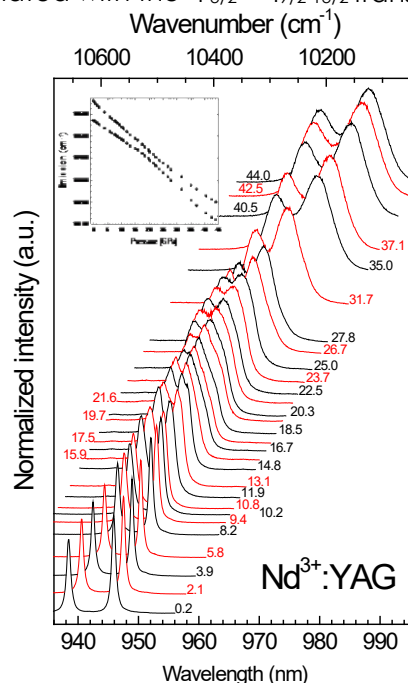


Fig. 2 R₁,R₂→Z₅ emission spectra associated with the Nd³⁺ $^4F_{3/2} \rightarrow ^4I_{9/2}$ transition as a function of pressure.

As an example, the pressure-induced shift of the emission spectrum corresponding to the near infrared $^4F_{3/2} \rightarrow ^4I_{9/2}$ transition of Nd³⁺ ions in a YAG crystal was obtained from ambient conditions up to 44 GPa in order to test its suitability as an optical pressure sensor. The R₁,R₂→Z₅ transitions are characterized and fit the requirements of an ideal optical pressure sensor.

References

[1] A. Yoshikawa, B.M. Epelbaum, K. Hasegawa, S.D. Durbin, T. Fukuda, J. Cryst. Growth 205, 305 (1999).

Keywords: Garnet; Luminescence; High Pressure

Full Name: Victor Lavin

E-mail: vlavin@ull.edu.es

Growth and characterization of $(\text{Lu}, \text{Y}, \text{Gd})_3(\text{Al}, \text{Ga})_5\text{O}_{12}:\text{Ce}; \text{Mg}$ crystals for timing application

Assoc. Prof. Weerapong Chewpraditkul, Dr. Ongsa Sakthong, Mr. Warut Chewpraditkul
King Mongkut's University of Technology Thonburi, Thailand

This report summarizes our research work during short research visit at Yoshikawa's Laboratory, Institute of Materials Research (IMR), Tohoku University, from June 13 to July 4, 2018.

The purpose of this visit was to grow $(\text{Lu}, \text{Y}, \text{Gd})_3(\text{Al}, \text{Ga})_5\text{O}_{12}:\text{Ce}; \text{Mg}$ multicomponent garnet crystals and characterize their scintillation properties. These crystals were grown by micro-pulling-down method.

1. Crystal growth and characterization

The garnet crystals of $\text{Y}_{0.8}\text{Gd}_{2.2}(\text{Al}_{5-x}\text{Ga}_x)\text{O}_{12}:\text{Ce}; \text{Mg}$ (YGdAGG:Ce;Mg) & $\text{Lu}_{0.8}\text{Gd}_{2.2}(\text{Al}_{5-x}\text{Ga}_x)\text{O}_{12}:\text{Ce}; \text{Mg}$ (LuGdAGG:Ce;Mg) with $x = 2.6$ and 3 were grown by the micro-pulling-down method using an RF heating system (Fig.1). The dopant concentration in the melts was 1 at.% Ce and 0.15 at.% Mg. An Ir crucible was used in the atmosphere of Ar + 2%O₂ to prevent evaporation of gallium oxide. The seed was GAGG:Ce crystal rod attached to the alumina seed holder. The pulling rate was 0.05 mm/min and the crystal diameter was around 4 mm. The photograph of as grown LuGdAGG:Ce;Mg crystal is shown in Fig. 2. The polished plates with thickness of 1 mm cut from the parent rods were used for all the measurements, i.e. X-ray induced radioluminescence (RL) spectra, scintillation decay time, light yield (LY) and thermoluminescence characteristics.

The RL spectra measurements were performed using CCD-coupled monochromator under excitation with X-ray tube (20 kV, 0.15 mA). Fig.3 shows the RL spectra of the μ -PD grown LuGdAGG:Ce;Mg crystal samples. The RL spectrum of Ga = 3 sample was slightly blue-shifted with respect to the sample with Ga = 2.6 was observed. It can be attributed to a



Fig. 1. Photograph of the μ -PD growth machine.

decrease in a crystal field strength around Ce^{3+} ion at the dodecahedral site from partial substitution of Gd^{3+} by the smaller Lu^{3+} ions, which causes a high-energy shift of the $5d_1$ level of Ce^{3+} center.

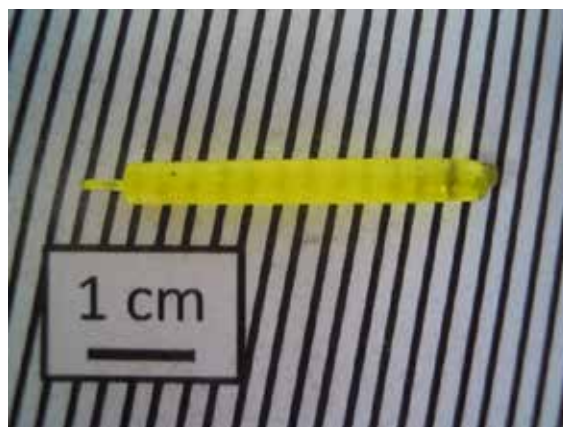


Fig. 2. Photograph of as-grown LuGdAGG:Ce;Mg crystal grown by the μ -PD method.

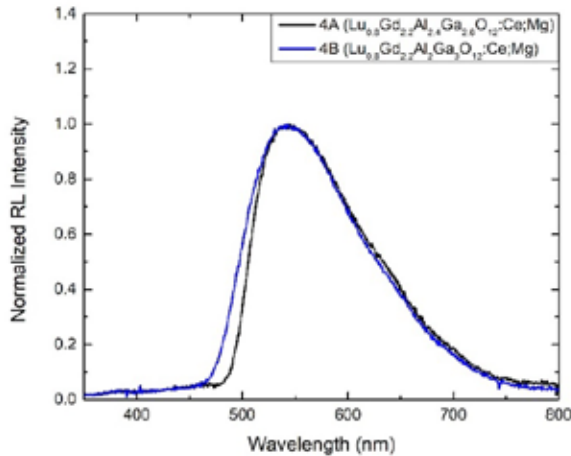


Fig. 3. RL spectra of LuGdAGG:Ce;Mg samples.

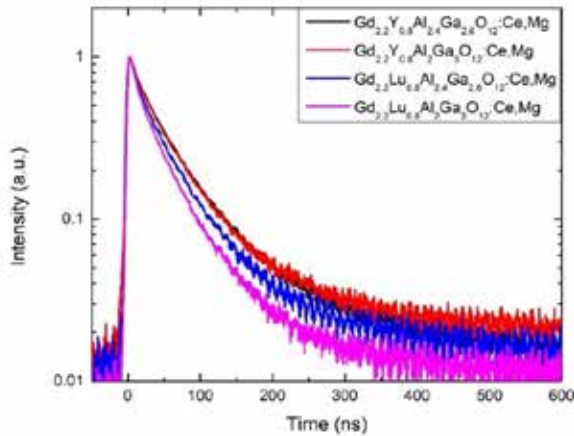


Fig. 4. Scintillation decays of LuGdAGG:Ce;Mg and YGdAGG:Ce;Mg crystals.

The scintillation decay time measurements were performed using a Hamamatsu R7600U-200 PMT and a Tektronix TDS3052 digital storage oscilloscope under excitation with γ rays from a ^{137}Cs source. Fig.4 presents the scintillation decay curves of LuGdAGG:Ce;Mg and YGdAGG:Ce;Mg crystals. The decay components and relative intensities were estimated by fitting the scintillation decay curves with a double - exponential function: $I(t) = \sum A_i \exp(-t/\tau_i) + \text{background}$, and the results are collected in Table 1. The LuGdAGG:Ce;Mg crystals show a faster decay time with respect to YGdAGG:Ce;Mg ones. The scintillation decay time was accelerated with increasing Ga content. It can be due to a blue-shifted emission spectra caused by a high-energy shift of the

$5d_1$ level upon partial substitution of Al^{3+} by a larger Ga^{3+} ions, which reduces the crystal field strength around Ce^{3+} ions at the dodecahedral site. Scintillation decay time for $\text{Gd}_3\text{Al}_2\text{Ga}_3\text{O}_{12}:\text{Ce};\text{Mg}$ is also included in Table 1 for a comparison.

Table 1 Scintillation decay time and relative intensity of YGdAGG:Ce;Mg and LuGdAGG:Ce;Mg crystals.

Crystals	τ_1 (I%) ns	τ_2 (I%) ns
$\text{Y}_{0.8}\text{Gd}_{2.2}\text{Al}_{2.4}\text{Ga}_{2.6}\text{O}_{12}:\text{Ce};\text{Mg}$	25 (28%)	81 (72%)
$\text{Y}_{0.8}\text{Gd}_{2.2}\text{Al}_2\text{Ga}_3\text{O}_{12}:\text{Ce};\text{Mg}$	20 (22%)	69 (78%)
$\text{Lu}_{0.8}\text{Gd}_{2.2}\text{Al}_{2.4}\text{Ga}_{2.6}\text{O}_{12}:\text{Ce};\text{Mg}$	16 (18%)	61 (82%)
$\text{Lu}_{0.8}\text{Gd}_{2.2}\text{Al}_2\text{Ga}_3\text{O}_{12}:\text{Ce};\text{Mg}$	12 (18%)	52 (82%)
$\text{Gd}_3\text{Al}_2\text{Ga}_3\text{O}_{12}:\text{Ce};\text{Mg}$ [1]	45 (41%)	108 (59%)

Light yield (LY) measurements were performed using a Hamamatsu R6231 PMT under excitation with a ^{137}Cs γ rays. To improve the light collection efficiency each sample was coupled to the PMT window with silicone grease and covered with several layers of Teflon tape. The signal from the PMT anode was processed by a CANBERRA 2005 preamplifier and a Tennelec TC243 spectroscopy amplifier set at 4 μs shaping time constant. Tukan 8 k MCA was used to record the pulse height spectra. The photoelectron yield (phe/MeV) was determined by relating the full-energy peak position with that of the single photoelectron peak from the PMT photocathode. Fig. 5 shows the pulse height spectra of γ rays from a ^{137}Cs source measured with the studied crystals. The LY(ph/MeV) values, calculated from the photoelectron yield using the quantum efficiency of PMT weighted over the RL spectrum, and energy resolution ($\Delta E/E$) are collected in Table 2. An increase of LY value with increasing Ga content (from 2.6 to 3) was obtained for both crystal hosts. It can be attributed to a decrease of bandgap energy (E_g), caused by more down-shift of the bottom of the conduction band with more substitution of Al^{3+} by a larger Ga^{3+} ions.

$\text{Y}_{0.8}\text{Gd}_{2.2}\text{Al}_{2.4}\text{Ga}_{2.6}\text{O}_{12}:\text{Ce};\text{Mg}$ shows highest LY value and best $\Delta E/E$ while $\text{Lu}_{0.8}\text{Gd}_{2.2}\text{Al}_2\text{Ga}_3\text{O}_{12}:\text{Ce};\text{Mg}$ exhibits lowest LY value but fastest scintillation decay time. The LY and $\Delta E/E$ for $\text{Gd}_3\text{Al}_2\text{Ga}_3\text{O}_{12}:\text{Ce};\text{Mg}$ [1] and $\text{Gd}_3\text{Al}_2\text{Ga}_3\text{O}_{12}:\text{Ce}$ [2] crystals measured under the

same experimental conditions are also included in Table 2 for a comparison.

Time resolution spectra of $Y_{0.8}Gd_{2.2}Al_2Ga_3O_{12}:Ce;Mg$ (YGAGG:Ce;Mg) and $Lu_{0.8}Gd_{2.2}Al_2Ga_3O_{12}:Ce;Mg$ (LGAGG:Ce;Mg) detectors measured in coincidence with a BaF_2 detector are shown in Fig. 6. An analysis of

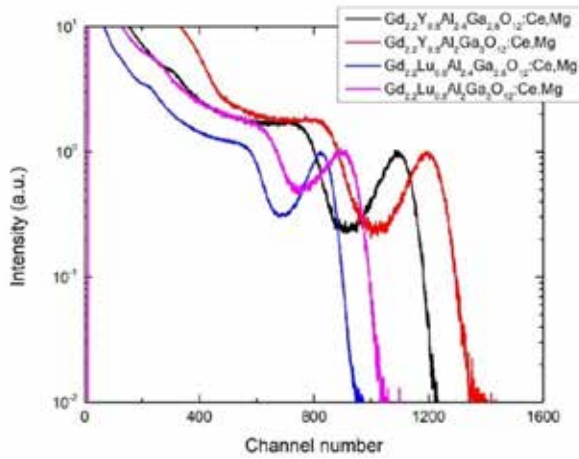


Fig.5. Pulse height spectra of ^{137}Cs γ rays measured for LuGdAGG:Ce;Mg and YGdAGG:Ce;Mg crystals.

Table 2 LY and $\Delta E/E$ of YGdAGG:Ce;Mg and LuGdAGG:Ce;Mg crystals.

Sample	LY (ph/MeV)	$\Delta E/E$ (%)
$Y_{0.8}Gd_{2.2}Al_{2.4}Ga_{2.6}O_{12}:Ce;Mg$	33,700	7.7
$Y_{0.8}Gd_{2.2}Al_2Ga_3O_{12}:Ce;Mg$	36,800	7.9
$Lu_{0.8}Gd_{2.2}Al_{2.4}Ga_{2.6}O_{12}:Ce;Mg$	25,400	8.3
$Lu_{0.8}Gd_{2.2}Al_2Ga_3O_{12}:Ce;Mg$	27,600	11
$Gd_3Al_2Ga_3O_{12}:Ce;Mg$ [1]	36,400	7.1
$Gd_3Al_2Ga_3O_{12}:Ce$ [2]	51,900	5.6

the measured time resolution is presented in Table 3. The time resolution (δ_t) in a second column is obtained after correction for a contribution of 128 ps time resolution of a BaF_2 detector. The third column shows the mean decay time (τ_m) defined by equation: $\tau_m = \Sigma(A_i\tau_i^2) / \Sigma(A_i\tau_i)$. The number of photoelectrons (N_f) measured at 0.5 μs time gate, is listed in the fourth column. The last column shows initial photoelectron rate (N/τ_m), a figure of merit in timing applications. Despite about 24% lower LY value, time resolution of LGAGG:Ce;Mg is slightly worse than that of YGAGG:Ce;Mg. This is mainly due to its faster

scintillation decay time, which leads to a comparable N/τ_m value.

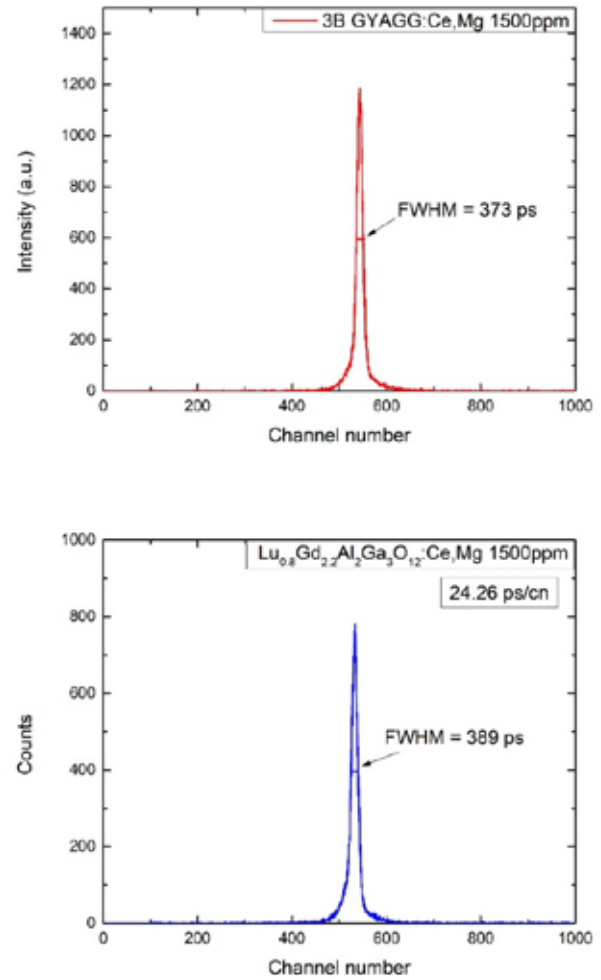


Fig. 6. Coincidence time resolution spectra of YGAGG:Ce;Mg- BaF_2 and LGAGG:Ce;Mg- BaF_2 detectors.

Table 3 Analysis of coincidence time resolution for $YGAl_2Ga_3G:Ce;Mg$ and $LGAl_2Ga_3G:Ce;Mg$ crystals coupled to an XP20D0 PMT.

Crystal	δ_t (ps)	τ_m (ns)	N (phe)	N/τ_m (phe/ns)
YGAGG:Ce;Mg	373	65	2120	33
LGAGG:Ce;Mg	389	50	1620	32

2. Co-Authored Publications

[1] W.R. Chewpraditkul, N. Pattanaboonmee, O. Sakthong, K. Wantong, W. Chewpraditkul, A. Yoshikawa, K. Kamada, S. Kurosawa, T. Szczesniak, M. Moszynski, V. Babin, M. Nikl, Scintillation

properties of GAGG:Ce;Li and GAGG:Ce;Mg single crystal scintillators: A comparative study, *Optical Materials* 92 (2019) 181–186.

[2] W.R. Chewpraditkul, N. Pattanaboonmee, O. Sakthong, W. Chewpraditkul, K. Kamada, A. Yoshikawa, M. Nikl, Scintillation properties of $Gd_3(Al_{5-x}Ga_x)O_{12}:Ce$; $x = 2.3, 2.6, 3.0$ single crystals, *Optical Materials* 81 (2018) 23–29.

[3] W.R. Chewpraditkul, N. Pattanaboonmee, W. Chewpraditkul, O. Sakthong, T. Szczesniak, M. Moszynski, K. Kamada, A. Yoshikawa, M. Nikl, Luminescence and scintillation characteristics of $(Gd_xY_{3-x})Al_2Ga_3O_{12}:Ce$; $x = 1, 2, 3$ single crystals, *Optical Materials* 76 (2018) 162-168.

3. Acknowledgments

I would like to thank all the members of Yoshikawa Laboratory and other Departments of IMR for their kind assistance and support.

June 2019

Keywords: Micro-pulling-down method; Scintillator;

Multicomponent garnet; Scintillation decays, Coincidence time resolution

E-mail: veerapong.che@kmutt.ac.th; ongsa.sak@kmutt.ac.th; raychew.rc@gmail.com

Spin-orbit torques in atomically-engineered metallic multi-layers

The spin-orbit interaction provides exciting opportunities to control spins by an electric means due to its relativistic nature. The generation of spin-orbit Hamiltonians can be governed by the symmetry of sample systems, such as by the crystalline lattice point group and by the local inversion breaking at an interface. This project's aim goes beyond these conventional concepts by attesting whether it is possible to generate any spin-orbit Hamiltonians from "artificial" lattice stacks.

The current state-of-the-art in thin-film growth technologies achieves layer-by-layer growth in many different film stacks. These technologies have underpinned the development of research fields, such as low-dimensional electron transport in III-V semiconductor epitaxial hetero-structures where the band engineering at the atomic scale plays an enabling role [1].

Here we will transfer this approach to the field of spin-orbit transport and nano-magnetism. We aim to grow metallic thin-film multi-layers with atomically-controlled thicknesses to manipulate the spin-orbit interaction. The spin-orbit interaction is a short-range interaction, hence requiring such a spatial modulation of that extreme length-scale.

With this final goal, the first step we took during this visit was to focus on the growth of candidate samples to achieve epitaxial growth of specific stacks. Ni-Pt multi-layers were found to grow epitaxially prior to this visit thanks to Dr Seki. Their growth conditions in relation to the film crystallography as well as magnetic properties were studied in detail. Successful samples (not yet with atomically-controlled thicknesses) were brought back to UCL, where we performed spin-transfer-torque ferromagnetic resonance (STT-FMR) to check if we can establish a methodology to characterise spin-orbit transport on these multi-layer samples. Below we summarise highlights from our research.

Fig.1 shows reflection high-energy electron diffraction (RHEED) patterns of epitaxial Ni /Pt multi-layers. Ni and Pt films can growth epitaxially on top of each other

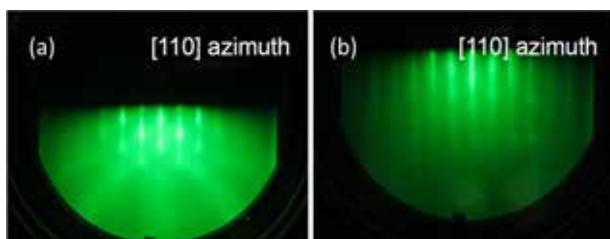


Fig.1: RHEED patterns taken after the growth of (a) the Ni and (b) Pt films. Both are taken along the [110] direction.

and can be a candidate of artificial lattice stacks used in this project. Magnetic properties were characterised by vibrating sample magnetometry (not shown).

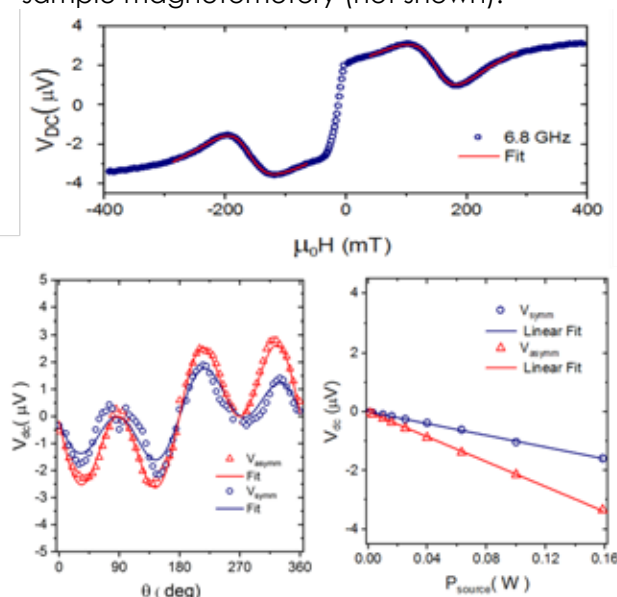


Fig.2: (a) FMR scan using the UCL STT-FMR set-up, together with a fit curve. The microwave frequency was set at 6.8 GHz. (b) Angle plots of both symmetric and anti-symmetric lineshape amplitudes (V_{sym} and V_{asym}) with model fit curves. (c) The power dependence of these amplitudes.

After the visit, STT-FMR experiments have been performed for these samples. Figure 2 displays a typical FMR voltage profile together with plots of the amplitudes as a function of angle and microwave power. These measurements can reveal magnetic properties (anisotropy and damping) and spin torque characteristics such as the spin-Hall angle.

During this short period of time, we rapidly combined our research strengths and demonstrated a promising start. This will act as a springboard for our primary research objective.

References

- [1] e.g. B. J. van Wees et al., Phys. Rev. Lett. 60, 848 (1988).
- [2] L. Liu et al., Phys. Rev Lett. 106 036601 (2011).

Keywords: spintronics, spin transfer, spin current
 Hidekazu Kurebayashi (University College London)
 E-mail: h.kurebayashi@ucl.ac.uk
<https://www.ucl.ac.uk/spintronics>

Spin Dimer Magnet $\text{SrCu}_2(\text{BO}_3)_2$ and Dioptase Minerals in High Fields

The goal of this project was to complete the high-field neutron scattering investigations of Shastry-Sutherland frustrated magnet $\text{SrCu}_2(\text{BO}_3)_2$ and prepare for the new neutron experiments in high magnetic fields under pressure. In addition systematic magnetization measurements in pulsed magnetic fields up to 30 T have been performed on a low dimensional magnetic system – natural gem crystal green dioptase and its dehydrated modifications blue and black dioptase.

The single visit program can be divided in three parts. The first one was dedicated to discussion of the results obtained on $\text{SrCu}_2(\text{BO}_3)_2$ (SCBO) in the previous neutron experiment in high fields and preparation for the next high-field neutron experiment under high pressure [1]. SCBO is one of the most prominent examples of coupled spin dimer magnet with strong frustration, a realization of Shastry-Sutherland system, which has stimulated a large number of experimental and theoretical investigations, see e.g. [2] and references therein. As a result of these discussions, a dedicated 1 GPa high-pressure cell compatible with a dilution cryostat of the 26T magnet at HZB has been designed as shown in Fig.1 The application of high pressure should allow reaching the first (1/3) magnetization plateau of SCBO at fields lower than 26T (see Schneider et al, Phys. Rev. B 93 241107 2016) which are accessible at HFM/EXED at HZB.

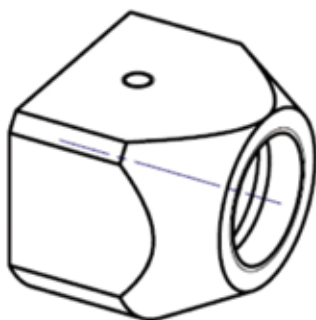


Fig. 1 High-pressure cell designed by Prof Uwatoko (ISSP, Kashiwa) for the HFM/EXED experiment on SCBO.

The second part was devoted to the magnetization measurements in pulsed fields up to 30 T on another quantum magnet – gem crystal of natural (green) dioptase (GD), $\text{Cu}_6[\text{Si}_6\text{O}_{18}]\cdot 6\text{H}_2\text{O}$, and its high-temperature dehydrated modifications blue (BD) and

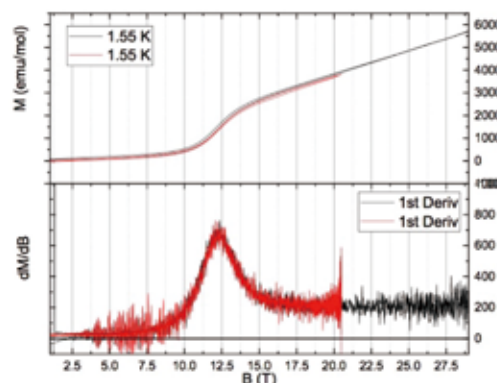


Fig. 2 High-field magnetization measurements (top) and (its first derivative) as function of magnetic field for green dioptase.

the c-axis of the hexagonal lattice and only one Cu in-plane neighbor forming a threefold spin-1/2 network. It is known that if a magnetic field is applied along the c-axis in GD there is a spin-flop transition around 13 T (Fig. 2) [4]. Nothing is however known about high field behavior of the BD and DD. We performed measurements for all three samples and could detect the spin-flop transition in GD at 12.5T and similar transitions in BD and DD appearing at lower fields [5].

Finally, following the recently signed MoU between Tohoku University and HZB, possible collaboration project have been discussed. They include common use of IMR instruments at JRR3 research reactor after its restart and development of pulsed magnetic field capabilities for synchrotron BESSY-II at HZB.

References

- [1] K. Kakurai et al, Research proposal HFM-191-00024 "Direct observation of spin superlattice under pressure and magnetic field in the Shastry-Sutherland system $\text{SrCu}_2(\text{BO}_3)_2$ "

Keywords: magnetic properties, high magnetic fields, neutron scattering

Full Name (Division Name or Affiliation)

E-mail: nojiri@imr.tohoku.ac.jp

<http://www.hfpm.imr.ac.jp/index.html>

Activity Report

Young Researcher Fellowships



[4] Young Research Fellowships

Application No.	Name	Host Professor	Proposed Research	Title	Affiliation	Term
18FS01	Maria Szlawska	Assoc. Prof. Honda	Investigations of Pressure Phase Diagram of Ce_3PdIn_{11} and Ce_3PtIn_{11}	Postdoctoral Fellow	Institute of Low Temperature and Structure Research, Polish Academy of Sciences, Wrocław, Poland	2018.5.12-7.1
18FS02	Denis Rybin	Prof. Kato	Structural Investigation of Nanoscale Detonation Carbon Obtained Using a Pulse Gas-Detonation Device	PhD Student	Lavrentyev Institute of Hydrodynamics, Siberian Branch of the Russian Academy of Sciences, Russia	2018.6.30-8.13
18FS03	Florian Jakobs	Prof. Bauer	Theoretical Investigation of Non-Equilibrium Intra-Atomic spin Transfer in Rare-Earth Atoms	PhD Student	Fachbereich Physik, Freie Universität Berlin, Germany	2018.7.28-9.5

Investigations of pressure-temperature phase diagram of $\text{Ce}_3\text{PdIn}_{11}$ and $\text{Ce}_3\text{PtIn}_{11}$

The electrical resistivity of antiferromagnetic heavy-fermion superconductor Ce_3PdIn_8 was measured under high pressure conditions. Both, the Néel and superconducting transition temperatures shift towards lower temperatures with increasing pressure.

The ground state of Ce-based compounds depends on subtle balance between Kondo and RKKY-type interactions. Both depend on the product $JN(E_F)$, where J is an exchange coupling between spins of electrons from $4f$ and conduction bands, and $N(E_F)$ is the density of states at the Fermi level. Thus, the ground state in Ce-based compound can be easily tuned by external parameter such as pressure, magnetic field or doping.

The Ce-based ternaries $\text{Ce}_3\text{PdIn}_{11}$ and $\text{Ce}_3\text{PtIn}_{11}$ crystallize with the tetragonal unit cell, strongly elongated along the c axis (space group $P4/mmm$), in which Ce atoms occupy two inequivalent crystallographic sites. Both compounds undergo two magnetic phase transitions at T_{N1} and T_{N2} into antiferromagnetically ordered state, and subsequent transition at T_C into superconducting state ($T_{N1} = 1.67$ K, $T_{N2} = 1.53$ K, $T_C = 0.42$ K and $T_{N1} = 2.2$ K, $T_{N2} = 2$ K, $T_C = 0.32$ K for $\text{Ce}_3\text{PdIn}_{11}$ and $\text{Ce}_3\text{PtIn}_{11}$, respectively) [1,2,3]. The complex ground states in both compounds may be attributed to the presence of two inequivalent Ce-atom sites in their unit cells. The Kondo and RKKY temperatures are expected to be different for both Ce positions, which may lead to coexistence of antiferromagnetism and superconductivity, yet occurring in two different sublattices [1].

In the framework of the project, the resistivity of $\text{Ce}_3\text{PdIn}_{11}$ was studied under high-pressure conditions, using Bridgmann pressure cells in He-free cryostat (between 1.3 and 300 K) and in dilution refrigerator (down to 130 mK).

The low-temperature dependence of the resistivity of the compound is presented in Fig. 1. The antiferromagnetic phase transition, marked with arrows, manifests itself as a tiny kink on the curve. It shifts towards lower temperatures with changing pressure from 0.15 to 0.9 GPa. The superconducting transition at 0.15 is quite broad and shows a step. At 0.9 GPa, the transition is broader and the step is more distinct. The resistivity measured at 2.2 GPa shows a kink near 200 mK, possibly of superconducting origin.

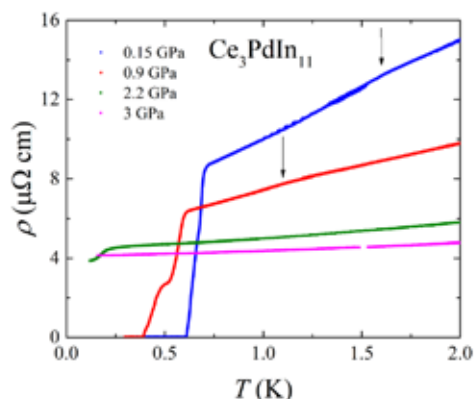


Fig. 1

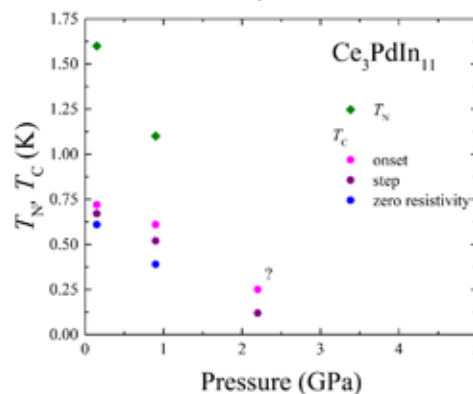


Fig. 2

The curve taken at 3 GPa does not show any singularity down to 150 mK. The preliminary p - T phase diagram of the system is shown in Fig. 2. It is highly important to continue measurements in order to gather more experimental data in the pressure window between 0.9 and 2.2 GPa.

References

- [1] M. Kratochvilová, et al., Sci. Rep. 5, 15904 (2015)
- [2] J. Prokleška, et al., Phys. Rev. B 92, 161114 (R) (2015)
- [3] J. Custers, et al. J. Phys.:Conf.Series 683, 012005 (2016)

Keywords: superconductivity, heavy fermion, electrical resistivity

Maria Szlawska (INTiBS PAN Wrocław, Poland), Fuminori Honda (Actinide Materials Science)

E-mail: m.szlawska@intibs.pl, honda@imr.tohoku.ac.jp

<http://www.intibs.pl> <http://www-lab.imr.tohoku.ac.jp/~aokilab/index.html>

Structural Investigation of Nanoscale Detonation Carbon Obtained Using a Pulse Gas-Detonation device

In this work, properties of nanoscale detonation carbon (NDC) which was produced in a Pulse Gas-Detonation Device (PGDD) by detonation of $C_2H_2+kO_2$ mixtures, with variation of k from 0.11 to 0.82 were investigated. Interaction of NDC with argon which used as an additive gas was studied. The structure of NDC which was obtained under various conditions of initiation of detonation such as various barrel length of detonation gun and various ratio of oxygen to carbon in initial mixture was investigated.

In experiments on detonation of rich acetylene-oxygen explosive mixtures in unsteady conditions, namely, upon detonation in tubes having an open end, it was found that under certain conditions, a black precipitate (carbon condensate) forms through of a chemical reaction between acetylene and oxygen. Based on these observations, a new method of obtaining nanoscale detonation carbon (NDC) was proposed [1]. In this method, the production of detonation carbon is conducted on a Pulse Gas-Detonation Device (PGDD) developed on the basis of a CCDS2000 detonation spraying facility. Using PGDD, experimental samples of NDC were produced using explosive mixtures having a molar ratio of oxygen to acetylene from 0.11 to 0.82. It was found that the structure, bulk density and the specific surface area of NDC depend on the oxygen concentration in the initial explosive mixture. The XRD analysis showed that there is a clear dependence of the content of graphitized carbon in the samples on the concentration of oxygen in the initial explosive mixture. The sample of NDC obtained at $O_2/C_2H_2=0.51$ has the highest content of the graphitized carbon.

Fig.1 shows XRD diagrams of NDC obtained at various molar ratios of oxygen to acetylene in initial explosive mixture.

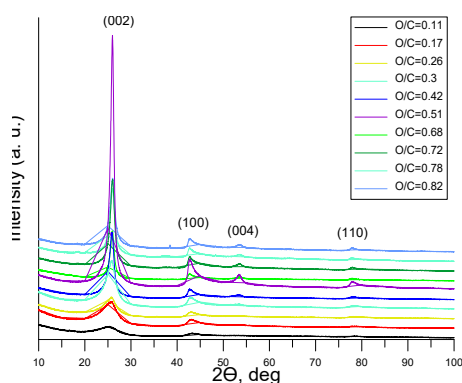


Fig. 1 XRD data of NDC samples

The morphology of the NDC samples was studied by Scanning Electron Microscopy. A dependence of the morphological characteristics of NDC on the composition of the explosive mixture was observed. Thus, at $O_2/C_2H_2=0.3$, carbon forms spheres with diameters of 20-100 nm. At $O_2/C_2H_2=0.51$, the diameter of individual spheres reaches 200 nm and sintering of the carbon particles to each other to form large agglomerates was observed. At $O_2/C_2H_2=0.68$, a transition occurs: the spherical particles disappear and graphene-like particles of complex (curved) shapes with a thickness of up to 20 nm appear. A further increase in the oxygen content in the initial explosive mixture does not lead to visible changes in the morphology of NDC.

Fig. 2 shows modification of morphology of the investigated NDC samples.

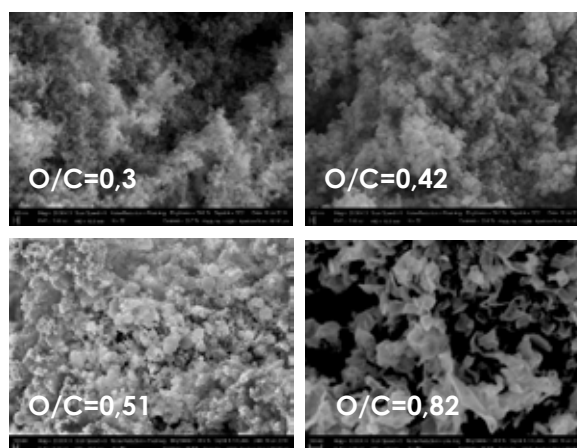


Fig. 2 Changes of the structure of NDC

The structure of NDC which was obtained under various conditions of detonation initiation of the initial explosive mixture was investigated. When argon was used as an additive and purge gas instead of nitrogen, it was found that the graphitization degree of NDC markedly increased only in the case of using argon as the purge gas. It's validated by Raman data: at $O_2/C_2H_2=0.42$

the ID/IG value in case of nitrogen equal 0.81, while for argon its equal 0.49.

Also influence of changing of geometry of PGDD on NDC structure was investigated. It was observed that Increasing of barrel length increases the graphitization degree of NDC. It's confirmed by Raman data: at $O_2/C_2H_2=0.68$ the ID/IG value in case of long barrel (L=1500mm) equal 0.29, at the same time in case of short barrel (L=750 mm) this value equal 0.51.

This investigation is extremely important from the point of view of understanding the process of graphitization of NDC formed during the detonation of rich acetylene-oxygen mixtures and the obtained data highlight promising directions for further research in this area.

References

[1] Shtertser A.A., Ulianitsky V.Yu., Batraev I.S., Rybin D.K. Production of Nanoscale Detonation Carbon using a Pulse Gas-Detonation Device // Technical Physics Letters. 2018. V. 44, No 5. P. 395-397.

Keywords: gas detonation, carbon, scanning electron microscopy (sem), x-ray diffraction (xrd)

Full Name Rybin Denis, Lavrentyev Institute of Hydrodynamics, Siberian Branch of Russian Academy of Science, Novosibirsk, Russia Federation
E-mail: rybindenis1990@gmail.com

Theoretical Investigation of Non-Equilibrium Intra-Atomic Spin Transfer in Rare-Earth Atoms

Atomistic classical spin dynamics have been used in the past successfully to describe the magnetization dynamics on short timescales. However, due to their intrinsic classical character, they fail at predicting some basic thermodynamic properties such as the specific heat of the spin system or the magnon power spectrum for a larger temperature range. We aim to implement and test a quantum thermostat to investigate non-equilibrium spin dynamics.

In the state-of-the-art experiments of ultrafast magnetization dynamics researchers are hoping to track the spin transfer between localized 4f and delocalized 5d6s spins in rare-earth materials. From a theory point of view, simulations are otherwise used to help interpret highly non-equilibrium experimental observations [1]. However, the classical spin dynamics simulations which are typically used have been shown to be deficient in describing the thermal statistics of magnons [2] (Fig. 1). Barker and Bauer have recently included a quantum thermostat in spin dynamics simulations to calculate equilibrium thermodynamics of magnetic materials [3].

In this research visit I aimed to learn about this technique, implement the method and eventually extend it to non-equilibrium scenarios.

Atomistic spin dynamics are based on a classical Heisenberg model and the numerical solution the Landau-Lifshitz-Gilbert equation for classical spins:

$$\frac{\partial \mathbf{S}_i}{\partial t} = -\frac{\gamma}{(1 + \lambda_i)} \mathbf{S}_i \times [\mathbf{H}_i + \lambda_i (\mathbf{S}_i \times \mathbf{H}_i)]$$

where \mathbf{S}_i is a spin at lattice site 'i', γ is the gyromagnetic ratio, λ is a damping factor and $\mathbf{H}_i = (1/\mu_{s,i})(\partial H/\partial \mathbf{S}_i) + \boldsymbol{\zeta}_i(t)$ is an effective field with $\mu_{s,i}$ as the magnetic moment, H the spin Hamiltonian and $\boldsymbol{\zeta}_i(t)$ is a stochastic field determined by the thermostat.

It is the stochastic thermostat term which we change to include quantum statistics, obeying the quantum fluctuation dissipation theorem

$$\varphi(\omega, T) = \frac{\hbar\omega}{\exp(\hbar\omega/k_B T) - 1}$$

The stochastic term must therefore have the correlations

$$\langle \boldsymbol{\zeta}_{i\alpha}(t) \rangle = 0$$

$$\langle \boldsymbol{\zeta}_{i\alpha}(t) \boldsymbol{\zeta}_{j\beta}(t') \rangle = 2\lambda_i \delta_{i\alpha} \delta_{j\beta} \varphi(t, t', T) / \mu_{s,i}$$

The difficulty in implementation comes from the fluctuation dissipation theorem being defined in frequency (ω) but the spin dynamics being solved in real time.

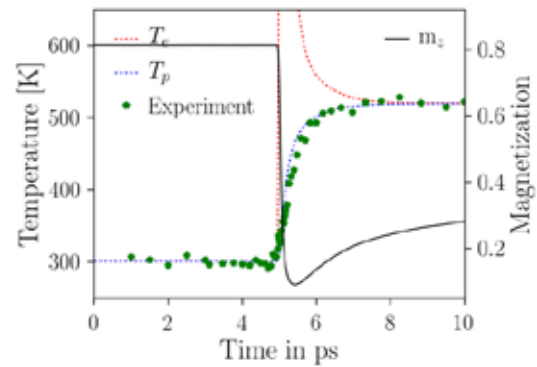


Fig. 1 A comparison of the phonon temperature and simulated ultrafast heating (electron, phonon and magnetization) of Ni using classical statistics. Although the comparison looks favorable, the extracted magnon specific heat is much too large.

We have now implemented the quantum thermostat and are performing calculations to test how it works in non-equilibrium situations with ultra-fast laser heating.

References

- [1] I. Radu, K. Vahaplar, C. Stamm et al., Nature, 472, 205 (2011)
- [2] M.D. Kuz'min, Phys. Rev. Letts., 94, 107204 (2005)
- [3] J. Barker and G.E.W. Bauer, arXiv:1902.00449 (2019)

Keywords: simulation, spin excitation
 Florian Jakobs (Freie Universität Berlin)
 E-mail: florian.jakobs@fu-berlin.de

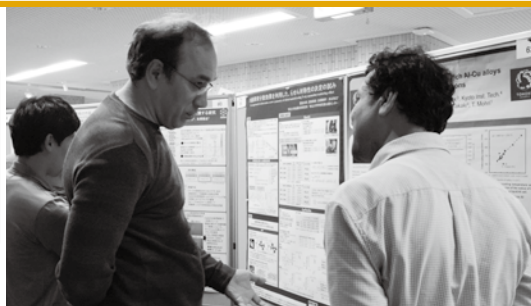
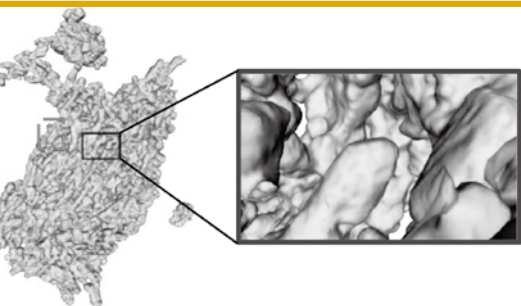
ICC-IMR FY2018 Activity Report

Edited by ICC-IMR Office
Published in August, 2019

Contact: International Collaboration Center,
Institute for Materials Research (ICC-IMR)
Tohoku University
2-1-1, Aoba-ku, Sendai, 980-8577, Japan
TEL&FAX: 81-22-215-2019
E-mail: icc-imr@imr.tohoku.ac.jp

Printing: HOKUTO Corporation

Copyrights © Institute for Materials Research



この冊子は「本なし印刷」
により印刷しております。



環境にやさしい「植物油インキ」
[VEGETABLE OIL INK]で
印刷しております。